Shigella flexneri Lipopolysaccharide Modifications in the Presence of Bile Salts

Ciara Bauwens

An Undergraduate Thesis
submitted to the Faculty of
the Department of Biology
in partial fulfillment of the requirements
for the degree of
Bachelor of Arts/Science in Biology/Biochemistry

Boston College
Morrissey College of Arts and Sciences
[May 2019]

Table of Contents

Acknowledgements

I would like to thank Dr. Christina Faherty for inspiring the ideas that went into this thesis, as well as giving me the opportunity to learn under her guidance. This research would not be possible without her continued help and support. I would like to thank Dr. Kourtney Nickerson, for helping me learn how to ask the right questions and for always being readily available for advice, resources, and reassurance.

I also owe a huge thanks to my fellow classmates and coworkers in lab: Dr. Meryl Perlman, Jaclyn Zois, Caitlin Ruane, Dennis Phan, David Le, Kathryn Nunes, Jessica Ding, and Kelvin Li for consistently helping, collaborating, and motivating me each day. I would also like to thank Dr. Doug Warner and Sandra Dedrick, as well as Dr. Momeni at Boston College, for their generosity and collaboration in sharing their lab space and equipment to facilitate my research.

To my Mom and Dad, none of this would be possible without your continued love and support, in both my academic and personal endeavors. Thank you for teaching me that with hard work and dedication, I can achieve my goals. Thank you to my brothers, Jim and Luke, for always having my back and making me laugh. Thank you to my Philly friends and Boston friends for your help, your advice, an unending loyalty during this time. I couldn't have done it without you all, and I appreciate you all so much.

Shigella flexneri Lipopolysaccharide Modifications in the Presence of Bile Salts

Ciara Bauwens

Advisor: Dr. Christina Faherty, Ph.D.

Shigella, a Gram-negative bacterial pathogen, induces inflammation and severe diarrhea by invading the colonic epithelium. Annually, millions of *Shigella* infections occur globally, mainly in children under five years of age in low-income communities. Despite years of research and multiple candidates, no effective vaccine exists against *Shigella*. This work centers on the importance of understanding the mechanisms of *Shigella* proliferation in the gastrointestinal tract before colonic infection, where an adverse environment is encountered and includes bile salts exposure, small intestinal components essential for digestion. *Shigella* is capable of resisting bile salts through mechanisms such as efflux pumps and biofilm formation. Another means of bile salts evasion is lipopolysaccharide (LPS) modification. LPS, comprised of the O-antigen, polysaccharide core, and lipid A, is a crucial outer membrane component for virulence. Transposon mutant analysis suggested a key role of *Shigella* LPS in bile salts resistance; thus, the goal of this study was to define *Shigella* LPS modifications following bile salts exposure. Three LPS mutants were investigated to distinguish crucial components of the LPS structure for bile salts resistance. All mutants were analyzed relative to wild type for growth in bile salts and biofilm formation. The LPS structures from wild type and the mutant strains were also purified and analyzed by polyacrylamide gel electrophoresis. Stained gels displayed modifications in the O-antigen, core components, and lipid A. Key bands were excised and sent for mass spectrophotometry sequencing. Results indicate that the O-antigen is a key regulator of *Shigella* bile salts resistance, as the complete O-antigen deletion mutant and both partial deletion mutants exhibited slow growth in bile salts and failed to form a biofilm in the presence of bile salts. This work highlights the importance of LPS changes for bile salts resistance and may help to improve vaccine development.

List of Abbreviations

1. ATP binding cassette (ABC) superfamily
2. Extracellular polymeric substance (EPS)
3. Gastrointestinal (GI)
4. Global Enteric Multicenter Study (GEMS)
5. Heptose residue 1 (Hep1)
6. Interleukin-8 (IL-8)
7. Lipopolysaccharide (LPS)
8. Luria Broth (LB)
9. Major facilitator superfamily (MFS)
10. Nuclear factor kappa-light-chain-enhancer of activated B cells (NF-κB)
11. Nucleotide-binding oligomerization domain-like receptors (NLRs)
12. O-antigen (Oag)
13. Peptidoglycan (PGN)
14. Polymorphonuclear cells (PMNs)
15. Random Amplifications of Transposon Ends (RATE)
16. Resistance nodulation division (RND) superfamily
17. Reverse transcriptase polymerase chain reaction (RT-PCR)
18. Tryptic Soy Broth (TSB)
19. Type 3 Secretion System (T3SS)
20. Wild type (WT)

Introduction

The bacterial pathogens of the *Shigella* genus cause a significant global public health burden. In 2015, the Global Burden of Disease Consortium recorded *Shigella* as the second leading cause of diarrheal mortality and the third leading cause of diarrheal deaths in children less than 5 years of age [32]. Despite a decline in *Shigella* infections over the last several decades, the burden of disease still affects communities around the globe, especially young children in developing countries. Of the 164,000 annual deaths caused by shigellosis, the species *Shigella flexneri* causes almost two thirds of the infections in low- and middle-income countries [34]. The bacteria spread from person-to-person via the fecal-oral route, in which transmission is exacerbated by inadequate sanitation and hygiene practices. Therefore, young children in developing countries are disproportionately affected.

Published in 2012, the Global Enteric Multicenter Study (GEMS) was an age-stratified case study to evaluate the burden and microbiologic cause of diarrheal disease in children aged 0-59 months in sub-Saharan Africa and South Asia. Of this age group, 25% of children in Africa and 31% in South Asia die due to diarrhea. These rates of childhood diarrheal death do not occur in wealthier societies [34]. The study investigated the clinical consequences of moderate to severe diarrhea by age, pathogen, symptoms, and location. The researchers also strove to discover the "antigenic and genotypic characteristics" of the most prominent pathogens in order to highlight potential vaccine targets, isolate risk factors, and create a well-maintained source of clinical specimens that can be shared among scientists to combat infectious disease [34]. Because enteric pathogens are a public health problem, group efforts such as this research study are essential to reducing the burden of diarrheal disease.

Shigella, a Gram-negative bacterial pathogen, causes shigellosis: bacillary dysentery inducing diarrhea, stomach pains, inflammation, and fever starting a day or two after exposure [10]. The *Shigella* genus comprises four species: *S. dysenteriae, S. sonnei, S. boydii, and S. flexneri* that are further divided into serotypes distinguished by the O-antigen (Oag) repeats of the lipopolysaccharide (LPS) molecules, a major component of the *Shigella* outer membrane [34]. Despite years of research, an effective vaccine remains elusive [41]. Furthermore, the presence of mutations and the acquisition of mobile genetic elements in the *Shigella* genome have led the bacteria to develop antibiotic resistance even within a decade of initial exposure, highlighting the importance of discovering an appropriate vaccine target. In 2019, the antibiotics of choice are ciprofloxacin, azithromycin, and ceftriaxone, yet resistance is emerging for these modern drugs as well [34].

One potential vaccine target is the LPS structure; however, the vast number of serotypes with varying Oag repeats has contributed to the failures of vaccine development. The GEMS found that of 1130 case isolates, *S. flexneri* comprised 65.9% that encompassed serotypes 2a, 6, 3a, 2b, and 1b [41]. *S. sonnei* is responsible 15% of infections in developing countries and 77% in industrialized countries, making it a key vaccine target as well. The researchers conclude that a quadrivalent vaccine with Oag from *S. sonnei*, *S. flexneri* 2a, *S. flexneri* 3a, and *S. flexneri* 6 serotypes could deliver broad coverage against the most common serotypes, and indirect coverage against remaining serotypes [41]. Because protection against *Shigella* is serotype specific, most *Shigella* vaccines target the epidemiologically significant serotypes. The inclusion of more serotypes in LPS-based vaccine formulations would require a more complex vaccine and a higher manufacture cost; but if type-specific antigens confer cross-resistance, the complexity can

be reduced. Live oral vaccines and Oag conjugated vaccines based on the immune response to Oag have been attempted to protect against *Shigella*, but these candidates have not provided sufficient protection [4].

Given the significance of the Oag and LPS in *Shigella* vaccine development, as well as the potential alterations of the LPS structure upon exposure to bile salts during small intestinal transit (see below), we sought to define important LPS modifications during bile salts exposure as a potential avenue to improve *Shigella* vaccine development. LPS, specifically the Oag, are critical components to vaccine development; however, the implications of bile salts to the creation of a suitable vaccine have not been investigated. Thus, this thesis tested the importance of LPS genes on the ability of the bacteria to modify the LPS structure and resist bile salts in culture conditions that mimic *S. flexneri* transit through the host gastrointestinal tract.

Literature Review

Shigella Pathogenesis

The *Shigella* species are facultative anaerobic, Gram-negative rod-shaped bacteria responsible for shigellosis, a disease in the large intestine or colon of human hosts. The bacteria must travel through the entire length of the digestive tract to reach the colon, where it can invade the epithelial cells lining the colon (**Figure 1**). Though the pathogen does not invade the stomach or small intestine directly, *Shigella* has multiple barriers to overcome in the gastrointestinal (GI) tract before it can infect the colon.

The human body has natural defenses in place to resist pathogens; however, *Shigella* employs several strategies to resist these defenses including alterations to the LPS structure. Resistance to colonization by foreign bacterial species is an essential component of the gut

microflora defense system for humans. Research investigating the impact of commensal bacteria on the ability of *Shigella* to invade is limited; however, the infectious dose of *Shigella* suggests mechanisms exist to overcome the commensal bacteria that compete for nutrients, oxygen, and space. The infectious dose of *Shigella* is as little as 10 to 100 bacteria, with about 500 bacteria on average [16]. Because so few organisms are required for disease, *Shigella* likely employs several pro-survival mechanisms against the thousands of commensal bacterial species in the GI tract [2]. Another likely pathogen defense system in the gut are colicins, plasmid-encoded proteins produced by bacteria in response to stressful conditions [23]. Colicins are often lethal to other bacterial strains, killing through four mechanisms including: inhibition of cell wall synthesis, formation of pores in the cytoplasmic membrane, restriction of protein synthesis, or deterioration of cellular DNA[23]. Because commensal *Escherichia coli* in the GI tract release colicins as a natural defense against enteric pathogens, *Shigella* likely has resistance mechanisms in place that potentially includes aspects of the LPS structure. One hypothesis of colicin resistance considers the length of the Oag polymer strands. In *E. coli*, also in the same *Enterobacteriaceae* family and evolutionarily similar to *Shigella*, the Oag may protect outer membrane protein receptors to provide resistance to colicin. The biological mechanism of the Oag conferring this resistance is unknown [23]. Short Oag (10-17 repeat units) and long Oag (16-28 repeat units) conferred resistance to colicin E2 [23]. However and interestingly, very long chains enabled colicin E2 to navigate between LPS molecules [23]. Further research is needed with regards to colicin resistance and in relation to *Shigella*, but the example highlights the potential LPS alterations employed by pathogens in the GI tract. As discussed below, LPS alterations are a key component to bile salts resistance. Finally, the Oag aids in the resistance to complement-mediated lysis [45], a mechanism of the host immune system [40]. Very long Oag units (over 80 repeat units) confer resistance to complement, a group of plasma proteins that target bacteria for phagocytosis and are activated by

bacterial components including the Gram-negative lipid bilayers of the outer membrane [27]. These results further highlight how bacteria have resistance mechanisms in place to alter the LPS structure as needed in which different Oag lengths could be produced depending on the protection needed in a specific environment of the GI tract.

Shigella invades the colonic and rectal mucosae via the M-cell, specialized antigen presenting cells of the GI epithelium [58]. The M-cells enable *Shigella* to cross the GI epithelial cell barrier and enter the subepithelial pocket (**Figure 1**). This intraepithelial pocket contains lymphocytes and macrophages, which attempt to initiate the mucosal immune response by phagocytosing the pathogen. However, *Shigella* disrupts the vacuolar membranes of the macrophages, enters and propagates into the cytoplasm, and causes cell death. *Shigella* is then released by the dying macrophage, which enables the bacteria to invade the colonic epithelial cells at the basolateral pole (**Figure 1**). The bacteria enter epithelial cells via membrane ruffling, actin rearrangements, and/or formation of protrusions using a set of virulence proteins that are secreted from the bacterial cytoplasm directly into the host cell by a needle-like complex termed the Type III Secretion System (T3SS). Following entry into the cytoplasm, bacteria replicate (**Figure 1**). Inside the host cytoplasm, *Shigella* move by prompting actin polymerization at one pole of the bacterium to propel the bacteria and establish cellular movement. This movement primarily occurs at tricellular junctions, the meeting of three cells [34]. At these locations, bacteria containing pseudopodia are taken up by neighboring cells, resulting in the intercellular spread of *Shigella.* The bacteria repeat these invasion steps multiple times, causing several infectious events during exposure [34]. Release of interleukin-8 (IL-8) recruits innate immune polymorphonuclear cells (PMNs), or neutrophils, to the site of infection. However, the PMNs weaken the integrity of the epithelial barrier and facilitate additional bacterial movement into the

subepithelial space. The PMNs eventually cause destruction of the tissue that is a hallmark of bacillary dysentery.

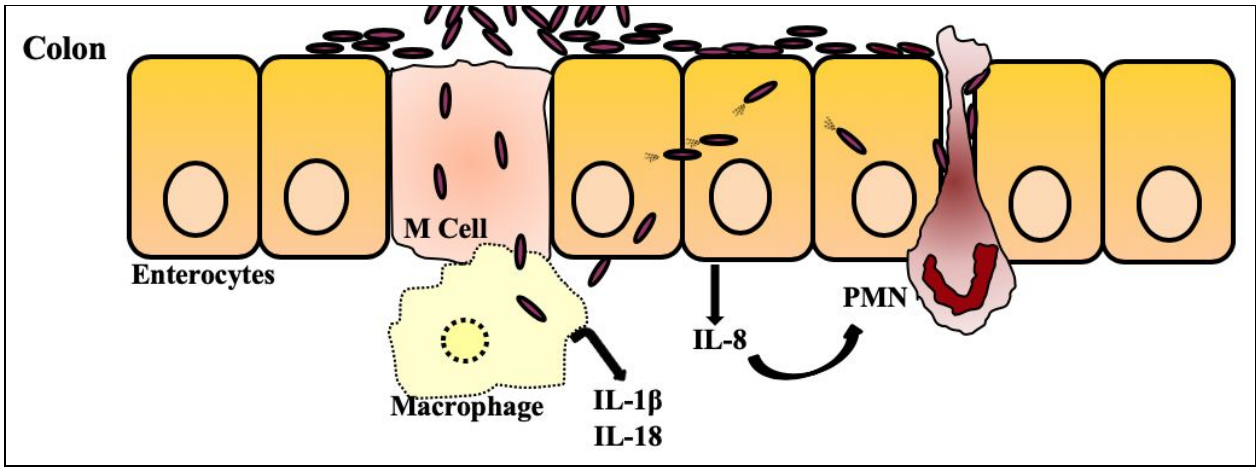

Figure 1. *Model of Shigella Pathogenesis***.** *Shigella* invades the colonic mucosae via M cells, which facilitate the bacteria crossing the epithelia. In the subepithelial pocket, *Shigella* disrupts the phagocytic membranes of macrophages, enters the cytoplasm, and causes macrophage cell death. The dying macrophage releases *Shigella*, which enables the bacteria to invade the colonic epithelial cells at the basolateral pole. During intracellular replication inside epithelial cells, the bacteria can spread to adjacent cells and control polymorphonuclear (PMN) cell migration (see text). Figure modified from (Nickerson, K. P., Chanin, R. B., Sistrunk, J. R., Rasko, D. A., Fink, P. J., Barry, E. M., Nataro, J. P. ,and Faherty, C. S. (2017). Analysis of *Shigella flexneri* Resistance, Biofilm Formation, and Transcriptional Profile in Response to Bile Salts. *Infection and Immunity*, *85*(6), 1–18).

Virulence Plasmid

Shigella flexneri contains several virulence genes, most of which are located on the virulence plasmid: a 220 kb extrachromosomal DNA replicon containing genes critical for pathogenesis [70]. The virulence plasmid includes the genes necessary to express an invasive phenotype. A 30 kb region on the virulence plasmid named "the entry region" contains the *mxi-spa* operon, which encodes the T3SS [74]. The T3SS is essential for cellular invasion, as it penetrates the host cell with a needle-like apparatus comprised of protein oligomers. The needle apparatus allows for the injection of virulence proteins that are vital to infection and intracellular

survival, and subvert the host innate and adaptive immune responses. The T3SS is also thought to communicate with environmental conditions, such as temperature, pH, or oxygen levels via a set of transcriptional regulators [45]. It is likely that crosstalk exists between the environment and T3SS, along with LPS and peptidoglycan modifications. Another operon on the plasmid is the *ipa* operon, which encodes invasion proteins required for entry into the host cells [47]. The virulence plasmid also encodes autotransporters of the Type V Secretion System, such as IcsA that polymerizes actin and enables the bacteria to spread to adjacent cells [45]. Autotransporters facilitate surface-localized proteins crossing the outer membrane in Gram-negative bacteria. These proteins recognize specific signal peptides of transport molecules, which are then cleaved during inner membrane transport [37]. In addition to the virulence plasmid, pathogenicity islands on the chromosome aid *S. flexneri* in infection. These transferable elements work with the plasmid virulence factors to invade the colonic epithelium [47].

Host Innate Immune Response

A key aspect of host cell immunity is programmed cell death in response to infection. The clearing of infected cells is essential for confinement of damaged tissue and inflammation, as well as presenting bacterial antigens to the adaptive immune system [3]. In general, when the bacteria enter the host, bacterial components such as LPS, peptidoglycan (PGN), and T3SS residues, are recognized by toll-like receptors (TLRs) on macrophages and dendritic cells to trigger the host immune response against *Shigella*. Intestinal epithelium expresses TLRs that provide an immune response against pathogens without inducing an inflammatory response that would otherwise break down the epithelial barrier. Dendritic cells and macrophages similarly can phagocytose bacteria without promoting an inflammatory response by secreting IL-10 [38]. The

PGN layer lies between the inner and outer membranes of *Shigella*. This layer provides additional support and cell structure, and also aids in anchoring proteins. The PGN is continually made and recycled, allowing the structure to change with changing environmental conditions. These changes are thought to confer resistance to antibiotics, protect from host enzymes that target the bacterial cell wall, and shield bacteria from immune system detection [25]. Nucleotide-binding oligomerization domain-like receptors (NLRs) in macrophages and dendritic cells are receptors that recognize bacterial PGN secretions. NLRs form inflammasomes, which are multi-protein signaling complexes [3]. Activation of inflammasomes results in the release of IL-1β and IL-18, as well as pyroptosis. Pyroptosis is a pro-inflammatory, lytic form of programmed cell death in macrophages that differs from apoptosis, a non-inflammatory programmed cell death [5]. *Shigella* can hijack the formation of the inflammasome and induce subsequent pyroptosis, resulting in bacterial escape from the macrophage to invade neighboring epithelial cells [3].

Although *Shigella* induces pyroptosis in macrophages, it prevents apoptosis caused by mitochondrial damage in epithelial cells. The T3SS virulence protein IpgD has multiple functions such as promotion of bacterial invasion and host cell survival, activation of epidermal growth factor receptor, and initiation of pro-survival signaling [3]. Unlike macrophage cell death that occurs within four hours of infection [58], *Shigella* uses several mechanisms to prevent host epithelial cell death including inhibition of mitochondrial damage, activation of cell survival signaling, and prevention of caspase activation and apoptosis [6]. Another T3SS virulence protein, *VirA*, promotes degradation of p53, blocking the pro-apoptotic pathway. *VirA* binds calpain inhibitor calpastatin, promoting bacterial entry while preventing apoptosis. Finally, *Spa15* prevents caspase-3 activation to help inhibit host cell apoptosis [13]. Eventually, the increased

calpain activation results in necrosis, which reduces bacterial proliferation. *Shigella* does exploit calpain activation to suppress innate immunity [3]. In all, these processes reveal that the bacteria control the balance of host cell death to facilitate survival and a replicative niche in epithelial cells.

Host Adaptive Immune Response

The body's adaptive immune response against *Shigella* consists of both systemic and mucosal responses against LPS and virulence plasmid proteins. Literature suggests that the host response targets the lipid A (endotoxic) component of LPS. Furthermore, *Shigella* infection experiments reveal serotype-specific immunity; and thus, a vaccine against one serotype will not necessarily confer immunity against another serotype. Antibodies have been found to provide some cross protection when made against common epitopes among Oag structures [39]. However, rectal biopsies of *Shigella* patients reveal widespread T and B cell deaths, suggesting that the bacteria weaken or evade cell-mediated immunity [3]. T cell activation and migration are essential for the induction of the adaptive immune response against bacteria. T cells have been found in the rectal mucosae of patients in the acute phase of shigellosis [36]. In general, T cell-mediated immunity in the GI tract includes cytotoxic T cells, intraepithelial lymphocytes, memory T cells in the lamina propria, and regulatory and helper T cells in Peyer's Patches [38]. B cells are also essential for antibody-mediated, or humoral, immunity by secreting antibodies that support the host response against bacteria. The host response includes release of serum antibodies IgG, IgM, and secretory IgA. Plasma cells, fully differentiated B cells, primarily secrete IgA into the GI lumen and represents the main contributor to gut adaptive immunity [39]. Secretory IgA binds the mucosal coating of epithelial cells, creating a protective antibody barrier in the lumenal pocket of the intestines [26]. The antibodies can also adhere to the outer membrane of bacteria, inhibiting

bacterial attachment to any mucosal surface in the gut. Furthermore, secretory IgA aids in antibody-dependent cell-mediated cytotoxicity, reducing the ability of bacteria to utilize growth factors [26].

The T cell response is limited during *Shigella* infection. First, it is proposed that T cells produce interferon gamma (IFN-γ) in response to *Shigella* infection, which increases macrophage activation and inflammation [36]. Furthermore, T cells have been found to produce IFN-γ as soon as four days following *Shigella* exposure, suggesting that these T cells could be memory cells from prior exposure or the result of cross-protection of T cells primed under a different infection, perhaps from a different serotype [36]. Second, there are also regulatory T cells in the gut to prevent inflammation against commensal bacteria and the breakdown of the gut epithelium by releasing IL-10, an important cytokine that can induce phagocytosis with limited inflammation.[38] The importance of IL-10 in *Shigella* infection has been highlighted by a clinical study. When volunteers were inoculated with invasive *Shigella dysenteriae*, 77% of participants had significant IL-10 production on day 0, and 87% had a significant increase in IL-10 production by day 28, measured by isolated peripheral blood mononuclear cells [62]. Third, *Shigella* can alter T-cell priming and motility [45]. *Shigella* can invade activated $CD4^+$ T cells and inhibit chemoattractant-mediated T cell migration by IpgD [3]. For a T cell to migrate, it depends on membrane cytoskeleton crosslinker proteins (ezrin, radixin, and moesin). IpgD (phosphoinositide phosphatase) can inactivate these crosslinker proteins [3] to prevent migration and reduce the host capacity for successful adaptive immunity. Finally, a key feature of T cell activation and the essential link between innate and adaptive immunity is impaired during *Shigella* infection. Antigen presenting cells, such as dendritic cells, present antigens to T cells for recognition. It is proposed that *Shigella* can downregulate chemokines that recruit dendritic cells, thus leading to reduced antigen presentation at the site of infection [66]. This blocking of dendritic

cells could lead to uncontrolled inflammation to facilitate *Shigella* invasion. Furthermore, it is hypothesized that this compromised antigen presentation leads to a reduced or improper T cell response; and thus, the reduced activation of memory cells and the prevention of the T cell-mediated response that is a hallmark of *Shigella* infection [66].

With regards to B cells during *Shigella* infection, several examples demonstrate disruption of normal B cell function. *Shigella* invades the B cell, reproducing intracellularly to kill the immune cell. The T3SS needle apparatus also can bind TLR2 on B cells, inducing apoptotic signaling in non-invaded B cells. This signal cascade enables *Shigella* to avoid antibody-mediated immunity [3]. However, some B cell function appears intact. Specific anti-LPS IgA has been found in shigellosis patients, and is hypothesized to protect against re-infection. Furthermore, anti-LPS IgA antibodies have been found in the breast milk of mothers exposed to *Shigella*, suggesting that this source of IgA protects the infant from infection [1]. IgG and IgM antibodies likely also play a role against *Shigella* LPS and virulence plasmid antigens, especially since T cell-deficient mice were resistant to wild type (WT) pulmonary *Shigella* due to anti-LPS IgM activity [73]. It is hypothesized that the serum antibodies are involved either in complement killing or antibody-dependent cytotoxicity. While promising, these antibodies have limited function. The Oag is "a carbohydrate, thymus-independent type 1 antigen" that activates B-cells in the absence of helper T-cells [47]. Without T-cell contribution however, the B-cells cannot develop a memory response to protect against reinfection by the pathogen. When a damaged bacterial cell releases LPS, the low concentration of type 1 antigens activates specific binding of B-cell receptors to the Oag, producing Oag- specific antibodies successful at protecting the host against *Shigella*. Thus, these antibodies are transient molecules and can be circumvented by serotype conversion or LPS modification. Conversely, an Oag on the bacterial surface of a healthy cell releases a high concentration of type 1 antigens. The high concentration of antigens

causes a "non-specific polyclonal activation of B cells", producing nonspecific antibodies that are less effective against invasion [47]. The Oag in this manner serves to confuse and circumvent the host immune system at several levels, making it an important consideration in the development of a successful *Shigella* vaccine.

Further Host-LPS interactions

Lipopolysaccharide is the major surface molecule of the Gram-negative outer membrane and impacts the virulence of most pathogens. LPS consists of three domains: the lipid A, or endotoxin, the core sugar component, and the Oag polysaccharide chains (**Figure 2**). The lipid A attaches to the outer membrane, and the Oag extends into the extracellular space. The Oag is a polymer of repeat units; the basic *S. flexneri* Oag consists of a tetrasaccharide of three rhamnose sugars and a single N-acetylglucosamine sugar [23]. The chain length of the Oag can confer different properties to the bacteria, as well as affect the virulence of the species. In general, bacterial adherence to the host epithelia may depend on the presence and length of the Oag chain [30]. Several cell receptors are capable of binding LPS, such as CD14 and TLRs. The TLRs are found on the basolateral membrane of the epithelium [58]. Mammals recognize LPS lipid A via the TLR4 surface receptor. Thus, the endotoxic lipid A component induces the innate immune response. TLR4 activation results in translocation of nuclear factor kappa-light-chain-enhancer of activated B cells (NF-κB), a transcription factor that increases the inflammatory response, into the nucleus. Once NF-κB reaches the nucleus, it promotes the expression of several pro-inflammatory cytokines including IL-6, IL-8, IL-1β, and more [45].

Finally, caspase-4/-11 activation is another attempt by the host epithelial cell to defend against *Shigella*. Typically in epithelial cells, caspase-4 and caspase-11 bind to cytoplasmic LPS,

activating caspase-4/-11-mediated pyroptosis [3], and causing epithelial cell shedding in order to eradicate infected cells. However, *Shigella* can hijack this inflammatory cell death pathway by the T3SS virulence protein OspC3, which promotes epithelial infection. OspC3 targets caspase-4, preventing activation. Thus, OspC3 cell death inhibition is important for bacterial infection by delaying host cell death to enable proliferation in surrounding cells. Because caspase-4/-11 binds LPS, it is important to understand its implications in evading the immune system, as the inactivation of caspase-4 is important for bacterial infection.

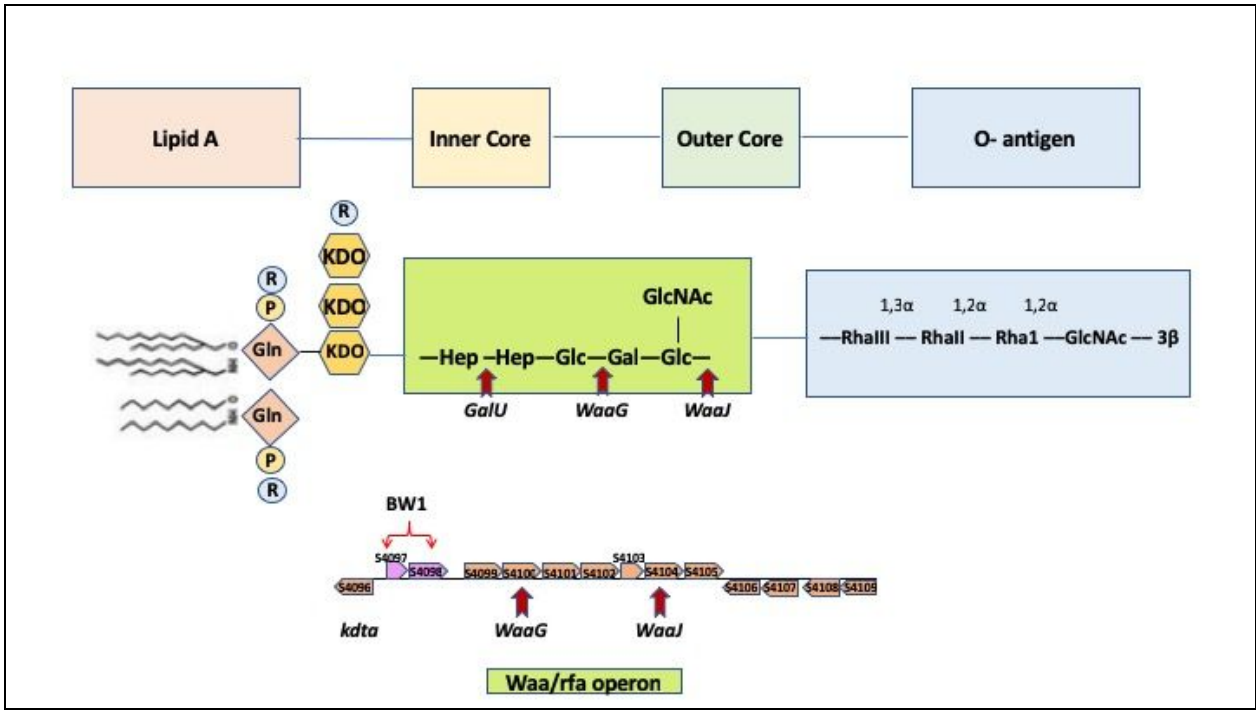

Figure 2. *Sample Lipopolysaccharide Structure*. The LPS consists of the lipid A, the polysaccharide inner core, and the O-antigen encoded by the *Shigella* genes in the *waa* or *rfa* operon. Core sugar residues and Oag units vary among serotypes. The *waaG, waaJ,* and *galU* gene deletion locations in the core structure and genome are highlighted with red arrows. *kdta* is the gene responsible for attaching the inner core to lipid A. BW1 refers to a transposon deletion mutant that was determined by DNA sequence analysis to disrupt genes S4097 and S4098.

Lipopolysaccharide and Infection

The Oag component of LPS is not necessary for survival; for example, rough *Shigella* mutants such as Δ*galU* that lack Oag side chains and can still cause infection. The *galU* gene, which encodes uridine triphosphate-glucose-1-phosphate uridylyltransferase, is involved in LPS biosynthesis. *galU* is responsible for the synthesis of uridine diphosphoglucose, a glucose molecule in glycosidic linkage with uridine diphosphate (Uniprot [68]). The Δ*galU* rough mutant has been found to invade HeLa cells, but is unable to generate membrane protrusions for cell:cell spreading [63] since the mutant improperly localizes the IcsA protein to the bacterial outer membrane. In strains with partial or missing Oag, IcsA localizes to the outer surface in a non-polar, or dispersed, fashion [58]. It is believed that LPS mediates IcsA polarity by creating "interlocking microdomains" with Oag side chains on the surface of the bacteria. These microdomains likely keep IcsA from disseminating away from one pole of the bacterial cell. The diffuse IcsA in LPS mutants polymerize the host cell actin, but the lack of cellular protrusions rendered the bacteria immobile in the cytoplasm [63]. Other rough *Shigella* mutants can invade cells but do not spread to adjacent cells, while strains with a smooth LPS containing an Oag improves virulence [24] via proper IcsA localization. These findings suggest that *S. flexneri* can express two Oag chain lengths that contribute to virulence in which short chains favor IcsA functioning while longer chains confer serum resistance [58].

Shigella has been known to reinfect the host with a different strain, perhaps via Oag serotype switching. This reinfection rarely occurs with a homologous serotype, but rather with a different one; enforcing the need for a vaccine that targets multiple serotypes [26]. The body produces antibodies against the LPS of *Shigella* that are serotype specific; and therefore, Oag

specific. The large variety of serotypes and thus LPS structures, as well as the fact that LPS antibodies are short-lasting, make it difficult to produce a targeted LPS antibody against *Shigella*. The adaptive immune response takes 4 to 7 days, but the persistence of *Shigella* after this time frame suggests that the bacteria subvert the immune system, either by changing the LPS arrangement or by avoiding effective immunological memory production [47]. The changing LPS structure suggests that an appropriate vaccine or antibiotic needs to be time specific (before the bacteria can modify LPS residues), or overarching among several variations of LPS residues.

The LPS may mediate host cell-bacterial interactions during this attachment and invasion. LPS is modified by glycosylation, which is believed to contribute to *S. flexneri* adhesion and therefore invasion. The presence of the SHI-O pathogenicity island on the chromosome includes genes for *S. flexneri* to modify LPS. The genes *gtrA* and *gtrB* in the *gtr* operon encode proteins for Oag modification and serotype conversion. It is hypothesized that *gtrX*, another glucosyltransferase in the *gtr* operon, positions the glucosyl group onto the Oag backbone; but, *gtrA* and *gtrB* assist in transportation of the glycosyl group [17]. It has been shown that glucosyltransferase mutants Δ*gtrA*$^{-}$ and Δ*gtrB*$^{-}$ had merely partial conversion of the Oag serotype, while a Δ*gtrX*$^{-}$ mutant had no conversion [47], suggesting that both *gtrA* and *gtrB* are necessary for full Oag conversion. This LPS conversion by glucosylation reduces the Oag length to enhance the ability of the T3SS to make contact with the host cell [47]. A mutation in the *gtr* operon diminishes the ability of the bacteria to invade the host epithelium, but the capabilities were restored when the operon was reintroduced.

Bile and LPS Interactions

The GI system produces various bactericidal agents, such as hydrochloric acid, bile, and other gastric secretions. These compounds create an acidic environment in the GI tract, with a pH of around 3.0 in the stomach [49]. This low-pH environment kills the majority of bacteria in the stomach, but the intestines have further defense mechanisms in place, such as bile; a fluid containing water, bile acids, electrolytes, cholesterol, bilirubin, and phospholipids that aids in digestion and fat absorption in the small intestine [47]. Bile also serves to eliminate waste products in feces. Bile acid, derived from cholesterol, degrades fat particles by increasing the surface area, allowing lipases to recognize the fatty acids. Bile acids can also form micelles, lipid aggregates that remain suspended in water, and are thus easily transported in an aqueous environment [69]. Both the emulsification and solubilization of lipid molecules are important for particle breakdown in the small intestine.

The liver metabolizes conjugated bile acids by attaching a glycine or taurine reside to the side chains of the bile acids. At physiological pH, conjugated bile acids are almost fully ionized and are termed bile salts. These salts remain in the gallbladder until circulation is stimulated by food intake [49]. Bile is then released into the duodenum, or upper portion of the small intestine, and maintained in the majority of the small intestine (the jejunum) to aid in digestion. Bile is absorbed in the terminal ileum, or end of the small intestine, so that only approximately five percent of bile enters the colon [61].

Since *Shigella* experiences long-term bile exposure, the bacteria have evolved to survive the bactericidal effects and manipulate bile as a host localization signal in order to regulate gene expression and prepare the bacteria for infection (**Figure 3**; [54]). Like other enteric pathogens [65],

Shigella can resist bile salts exposure [54]. Mechanisms that evade the bactericidal effects of bile salts include changes to the outer surface, use of efflux pumps, and biofilm formation, a common response in bacteria to survive stressful environmental conditions. A biofilm consists of bacterial attachment to a surface or aggregates of bacteria attaching to one another, coupled with extracellular polymeric substance (EPS) matrix secretion that consists primarily of polysaccharides and provides a protective coat over the bacteria [19]. During biofilm formation, bacteria alter gene adhesion expression profiles to enable and strengthen attachment. Typically, bacteria within a biofilm are slow-growing to decrease energy expenditure, reducing the efficacy of most antibiotics [19]. After the stressor is removed from the environment, the bacteria resume a planktonic, mobile lifestyle. For *Shigella,* a proposed model based on experimental data suggests that bile induces biofilm formation in the jejunum, which the bacteria then disperse in the terminal ileum when bile is recycled into circulation (**Figure 3**; [54]). Simple sugars such as glucose are available for bacterial utilization in the small intestine; hence both bile salts and glucose are important signals for *Shigella* biofilm formation [65]. It is hypothesized that the bile salt-induced biofilm is more transient compared to traditional, chronic biofilms in which gene transcription and bacterial proliferation slows. Both the rapid bacterial dispersion from the biofilm as *Shigella* transitions to the colon and the enhanced virulence gene expression observed within the biofilm population would result in this transient nature [65].

Another alternative mechanism bacteria have against bile salts are efflux pumps, specifically the ATP binding cassette (ABC) superfamily, the major facilitator superfamily (MFS), and the resistance nodulation division (RND) superfamily. Efflux pumps consist of transporter proteins which aid in resistance to stressful conditions, such as antibiotics and bile

salts [56]. Efflux pumps can expel a wide range of antibiotics and other toxic substances from the cytosol of the bacteria; therefore, efflux pumps have been linked to multidrug resistance. Efflux pumps have been shown to act as virulence factors in similar enteric pathogens, such as *Salmonella typhimurium, Listeria monocytogenes,* and *Vibrio cholera* [56]. It has been found that *Shigella* increases expression of the AcrAB efflux pump, which is a member of the RND family, in the presence of bile salts [54]. AcrAB extrudes dyes, detergent, and a variety of antimicrobials such as chloramphenicol and erythromycin [67]. Bile salts increases the transcription of the *acrAB* operon, and a Δ*acrB* mutant showed hypersensitivity to bile salts. This increased AcrAB efflux pump expression could aid in *Shigella* resistance to other therapeutics by "priming" the bacteria for an antibiotic resistance phenotype, so any antibiotics present will also be effluxed out of the bacteria [54]. *Shigella* have more than one resistance mechanism in place to avoid the effects of a stressful environment, so it is important to consider all aspects of potential compensations the bacteria make during long-term exposure to bile salts.

Finally, for many pathogens, outer surface changes in response to bile salts induce alterations to membrane proteins and LPS [65]. In *Salmonella typhimurium*, very long Oag chains with 80 repeat units confer resistance to bile salts, while shorter Oag chains do not confer such resistance [23]. Interestingly, Oags between 16 and 28 repeat units also impaired growth in bile, suggesting that different lengths of LPS Oag serve different functions in pathogenesis. The long Oag may interfere with enterobacterial common antigen-mediated bile resistance, while the very long chains could have different polysaccharide interactions to enable resistance [23]. Any modifications of *Shigella* LPS remain to be determined.

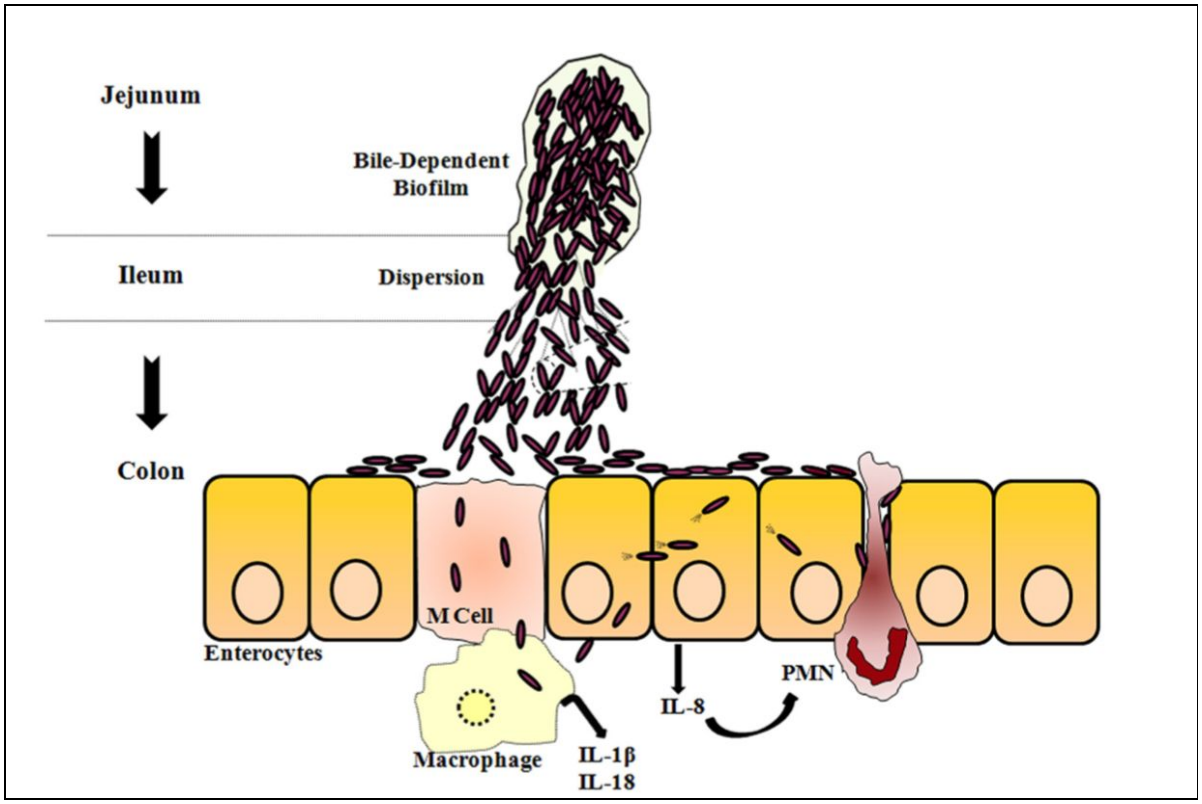

Figure 3. *The expanded Shigella infection paradigm***.** *Shigella* experiences long-term bile exposure en route to the colon. Bile aids in digestion and fat absorption, and is a bactericidal agent to most bacteria. *Shigella* has adapted to survive the bactericidal effects of bile salts, which include the formation of a biofilm as the bacteria transit the jejunum of the small intestine. In the terminal ileum, *Shigella* disperse the biofilm as bile is recycled into circulation, enabling a hypervirulent bacteria to infect the epithelial cells lining the colon. Figure modified from (Nickerson, K. P., Chanin, R. B., Sistrunk, J. R., Rasko, D. A., Fink, P. J., Barry, E. M., Nataro, J. P. ,and Faherty, C. S. (2017). Analysis of *Shigella flexneri* Resistance, Biofilm Formation, and Transcriptional Profile in Response to Bile Salts. *Infection and Immunity*, *85*(6), 1–18).

Objectives

LPS is a key outer membrane structure that has significant roles in infection and is a prime vaccine target. Based on the modifications seen in *Shigella* in response to bile salts [54 23], as well as the role of LPS in bile salts resistance for other pathogens [31 49 53], the goal of this thesis was to define the LPS modifications in *Shigella* following bile salts exposure. After identifying transposon insertion sites in mutants with reduced ability to resist bile salts and form a biofilm,

several mutants were associated with disruptions in LPS biosynthesis genes. The central focus of this thesis developed to begin to characterize LPS modifications in *S. flexneri* following bile salts exposure. It was hypothesized that *Shigella* modifies the LPS, specifically the number and orientation of Oag repeat residues as a mechanism to endure the bactericidal effects of long-term bile salts exposure during small intestinal transit. In order to investigate this hypothesis, LPS mutants with varying Oag and outer core lengths were created and/or investigated for bile salts resistance. LPS extraction analysis revealed that bile salts exposure results in a modified Oag, as well as a modified lipid A, inner core, and outer core in WT bacteria and the tested mutants. All mutants had delayed and reduced growth in bile salts compared to WT bacteria; and furthermore, were unable to form a biofilm. In all, this work improves our understanding of *Shigella* resistance in bile salts and may help to improve vaccine development.

Materials and Methods

Bacterial strains, plasmids, media, and growth conditions.

Table 1 summarizes the bacterial strains and plasmids used in this study. *S. flexneri* cultures were routinely grown in shaking conditions with aeration at 37° C in Luria broth (LB) or tryptic soy broth (TSB). TSB contains an additional 2.5 g/liter glucose relative to LB. Cultures of 3 mL or 10 mL were used depending on the protocol. After approximately 18 hours, the cultures were centrifuged for 10 minutes at 4000 rpm at 4° C and resuspended in the same volume of LB or TSB broth with or without 0.4% weight/volume bile salts, which consists of a 1:1 mixture of cholate and deoxycholate (Sigma). All media were filter sterilized with a 0.22 μm filter following the addition of bile salts. The cultures were standardized using an optical density

reading at 600 nm (OD_{600}) before the LPS extraction, growth, and biofilm assays. Bacteria were routinely maintained on TSB agar plates with 1.5% agar and 0.025% Congo red (CR; Sigma), an indicator dye used to confirm the virulence of the *S. flexneri* strains [48]. Transposon (BW) mutants were maintained using a kanamycin concentration of (50 μg/mL), while the Δ*waa* mutants were selected on plates using chloramphenicol (5 μg/mL). Ampicillin for plasmid maintenance was used at 100 μg/mL.

Table 1. Strains and Plasmids

Strain or Plasmid	Description	Source
2457T	*S. flexneri* serotype 2a	Source 15
Plasmid pKM208	Temperature-sensitive *red*-, *gam*-, *lacI*-expressing plasmid driven by *pTac* promoter, *bla*	Source 72
BS766	2457T + pKM208, ampicillin resistance	Source 48F
Plasmid pKD3	*oriR6K, bla, cat*	Source 72
BW1	2457T/*kdta/waaA*::Tn*5*, kanamycin resistance	This study
BW 3/4	2457T/*yohH*::Tn*5*, kanamycin resistance	This study
BW7	2457T/*malM*::Tn*5*, kanamycin resistance	This study
BW10	2457T/*ydjE*::Tn*5*, kanamycin resistance	This study
BW14	2457T/*ydiJ*::Tn*5*, kanamycin resistance	This study

BW 21	2457T/*rfbG*::Tn*5*, kanamycin resistance	This study
Δ*galU*	2457T/*galU::*Tn10; tetracycline resistance	Sources 17, 54
Δ*waaG*	2457T/*waaG::cat*, chloramphenicol resistance	This study
Δ*waaJ*	2457T/*waaJ::cat*, chloramphenicol resistance	This study

The Transposon Strategy for Creating Knockouts

The EZ-Tn5 transposon kit (Epicentre™) was used according to manufacturer's instructions for the creation of a library of mutants with random insertions of transposons into the *S. flexneri* genome. The transposon contains an antibiotic resistance gene (kanamycin) as the selectable marker. The insertion sites of the transposon in the mutants were determined using a multi-round PCR protocol termed Random Amplifications of Transposon Ends (RATE) [21] with some modifications. A primer specific to the end of the transposon (Inv-1 or Inv-2) was paired with a random hexamer primer for the PCR reaction (**Table 2**). Resulting amplicons were gel purified and sequenced using a second transposon-specific primer (KAN-2 RP-1 or KAN-2 FP-1, respectively). Following sequence analysis (Genewiz) to identify the portion of the *S. flexneri* genome amplified in the reaction, a second confirmation PCR reaction was performed using unique sequence-specific primers (**Table 2**) that annealed to the target region of the *S. flexneri* genome. An increased PCR product size in the mutant relative to WT bacteria corresponded to the size of the transposon, thus confirming the insertion site.

Plasmids and construction of mutant strains.

Deletion mutants were constructed using the ƛ red linear recombination method in which an antibiotic resistance cassette replaces the target gene through homologous recombination [72]. Transformations were performed using standard electroporation methods. Transformants were selected on agar plates containing chloramphenicol (5 µg/ mL). The deletion primers used have approximately 50 bp of 5' homologous overhangs to the upstream and downstream regions of the target gene of interest (**Table 2**; regions of homology to the antibiotic cassette are underlined). The primers amplify a chloramphenicol resistance cassette with homologous overhangs to the gene of interest. Following electroporation of the PCR cassette into a strain of WT 2457T harboring plasmid pKM208 that encodes the ƛ bacteriophage *gam, beta,* and *exo* genes, homologous recombination replaces the target gene with the antibiotic resistance cassette. Due to the temperature sensitivity of pKM208, the plasmid is lost during procedure, and the subsequent selection of transformants on chloramphenicol selects for the mutants.

Mutants are confirmed with a set of confirmation primers that detect a size shift in PCR products of the mutants relative to WT bacteria (**Table 2**). The Δ*waaG* and Δ*waaJ* mutants were created using this procedure. The *waaG* gene encodes LPS alpha1,3-glucosyltransferase (formerly known as lipopolysaccharide core biosynthesis protein RfaG) that aids in the addition of the first glucose residue to the LPS core (NCBI [52]). The *waaJ* gene encodes UDP-glucose:(galactosyl) LPS alpha1,2-glucosyltransferase that adds glucosyl residues to the LPS core backbone (Kegg [29]). In order to obtain template DNA for the confirmation PCR reactions, single colonies of WT and each of the chloramphenicol-resistant colonies from the mutation procedure were inoculated into 25 µL of 0.5M sodium hydroxide (NaOH) and

incubated at room temperature for 30 minutes. The reaction was neutralized with 25 µL of 0.5M Tris-HCl. The samples were diluted with 450 µL of sterile water. Subsequently, 2 µL of the reactions were used as template DNA for the PCR reactions.

Table 2. Primers used in the study.

Primer Name	Sequence
Inv-1	5'-ATGGCTCATAACACCCCTTGTATTA-3'
Inv-2	5'-GAACTTTTGCTGAGTTGAAGGATCA-3'
KAN-2 FP-1	5'-ACCTACAACAAAGCTCTCATCAACC-3'
KAN-2 RP-1	5'-GCAATGTAACATCAGAGATTTTGAG-3'
CAT - FP	5'-CATATGAATACCTCCTTAG-3'
CAT - RP	5'-GTGTAGGCTGGAGCTGCTTC-3'
WaaG deletion FP	5'-TGTTCGGGTTTATACCCAGTCGTGGGAAGGCGAATGCCCTGATGTATTTGCATATGAATACCTCCTTAG-3'
WaaG deletion RP	5'-ACCCGTTATGATATCCGCCGCTTTCTCTGGCAGACTGTATAAATCTTGTGGTGTAGGCTGGAGCTGCTTC-3'
WaaJ deletion FP	5'-TTTAAACATCTTACTCAATTTAAAGATATAATTGAACTGGACAAGCGCCCCATATGAATACCTCCTTAG-3'
WaaJ deletion RP	5'-TAATCTGCAGAGGCGTAGTTCGCCCAATCATGCCATGGCTTAGTTATACCGTGTAGGCTGGAGCTGCTTC-3'
WaaG CP FP	5'-GGCGTCCCTGGTCAAATAAC-3'
WaaG CP RP	5'-CGCCATTTCAAAGCGCAGAG-3'
WaaJ CP FP	5'-GTCTGGCGATCCTCATAAAG-3'
WaaJ CP RP	5'-TACGCTGAGCAACCTGATAC-3'
BW1 CP FP	5'-GTAGAGAAGGGCGGTGTAAAG-3'

BW1 CP RP	5'-CGGGATGGTGTCCTGATAAAG-3'
BW7 CP FP	5'-GATGGATAAAGATGCGCAGGG-3'
BW7 CP RP	5'-CCATCGAGATCTTCATTCCC-3'
BW14 CP FP	5'-TTCTTCAGGGCGATTCGATGTG-3'
BW14 CP RP	5'-CGGTGCTCATTGCGATTCTTTC-3'

*FP- forward primer, CP- confirmation primer, RP-reverse primer
++ Underlined primers were designed by Faherty lab members

Purification and Visualization of LPS

In order to isolate and visualize the LPS structure, the hot aqueous-phenol extraction method was used as previously described [12]. This protocol ensures that only LPS and potential sugar residues remain after the whole cell extract is processed with DNase, RNase, Proteinase K, detergent, and Tris-HCl to remove nucleic acids and proteins. The resulting LPS samples can be separated using an SDS-PAGE gel and stained, or transferred to a membrane and subjected to immunoblotting. The Pierce™ Color Silver Stain Kit (Thermo Scientific™) was used to stain the LPS residues using a weakly acidic silver nitrate solution for gel saturation, followed by development in alkaline formaldehyde. This silver stain produces visible bands of black, brown, blue, yellow, and red (Pierce Biotechnology™). The color patterns represent different molecular weight and charges of residues, and work to distinguish bands of similar size in the gel. The colorimetric silver stain produced the best results on a 4-20% Tris-Glycine gradient gel (Criterion™).

Gel images were captured using a fluorescent white light box and a digital camera, with images enhanced using photoshop. Key bands were excised and sent for mass spectrophotometry

sequencing. Gel analyses were performed by locating and counting Oag repeat bands and noting the size, shape, color, location of core and lipid A components [12]. Silver stain results can be seen in (**Figures 6, 7, 8 and Tables 4, 5**).

Growth Curve Assay

Following resuspension of overnight cultures in the test media, 130 µL of each bacterial culture was plated in a 96-well plate. Cultures were first standardized to the same OD_{600} reading to reduce variability in cell number between strains or treatments. Each strain was grown in LB, LB + 0.4% bile salts, TSB, and TSB + 0.4% bile salts. OD_{600} readings were taken at ten minute intervals by an Epoch2 microplate reader (BioTek™) to evaluate the impact of bile salts on the growth of each mutant and WT strains (**Figure 9**). For bile salts media, three independent experiments were used, with at least three technical replicate wells per strain and growth media per experiment. For TSB and LB media, two independent experiments were used, with at least three technical replicates. A two-way ANOVA test was used to calculate the statistical significance of the growth curve analyses.

Biofilm Solid-Phase Adherence Assay

The biofilm assay was performed as previously described [55] with slight modifications. Following the 1:1 replenishment of the culture media as described above, 130 µL of each bacterial culture were plated in a 96-well tissue culture-treated plate. TSB was used as the biofilm negative control media and TSB + 0.4% bile salts were used in the experimental wells. Following an overnight incubation, the OD_{600} was recorded to measure growth of the bacterial

strains. Subsequently, the media were removed, and the plate was washed once with 1X PBS and then dried. The bottoms of the wells were not disrupted, and any precipitate was left undisturbed during the washing. After drying, 0.5% crystal violet stain was added to each well and incubated for five minutes at room temperature. Following washes in distilled water, the plate was dried. To quantify the total biomass of the biofilm, the wells were resuspended in 95% ethanol, and the OD_{540} was measured. Biofilm assays were performed with two biological replicates, with a total of 11 technical replicates. Media control wells were used to ensure only bacterial growth was present in the inoculated wells. A two-way ANOVA test was used to determine the statistical significance of the results (**Figure 12**).

Results

Transposon Mutant Analysis

A library of mutants was previously created with random transposon insertions into the *S. flexneri* genome. Mutants with reduced abilities to grow in bile salts and/or form a biofilm were selected for analysis. This work began with the procedure of identifying the insertion sites of the transposons by using a multi-round RATE PCR protocol with some modifications [21]. PCR products were gel purified and sent for sequencing (Genewiz). Following identification of the transposon insertion site by sequence analysis (**Table 3**), a second confirmation PCR reaction was performed with primers that annealed to the target region of the genome to produce an increased PCR product size relative to WT *S. flexneri,* which corresponded to the size of the transposon and thus confirming the insertion site (**Figure 4**). Mutants BW1, 7, and 14 were confirmed using this method. BW3, BW4, BW10, and BW21 still require confirmation analysis.

Table 3. Transposon Mutant Identification

BW	**Phenotype from Transposon Screen**	**Genes Affected (locus; name)**	**Function**
BW1	**Slow growth in bile salts**	**S4097 and S4098; insertion sequences**	**Disrupting intergenic region between *kdta* and *waaQ***
BW 3/4*	Slow growth in bile salts	Upstream of S2353; *yohH*	MdtQ multidrug resistance transporter
BW7	Slow in bile salts, reduced early biofilm	S3563; *malM*	Maltose region periplasmic protein
BW10*	Slow growth in bile salts, low early biofilm	S1563; *ydjE*	MFS Transporter, transmembrane transporter
BW14	Slow growth in bile salts, low early biofilm	S1565; *ydiJ*	Fructose-biphosphate aldolase
BW21*	**Slow growth in bile salts**	**S2220; *rfbG***	**dTDP-rhamnosyl transferase**

* Asterisks indicate mutants that have not yet been confirmed
Bold font indicates genes associated with LPS biosynthesis

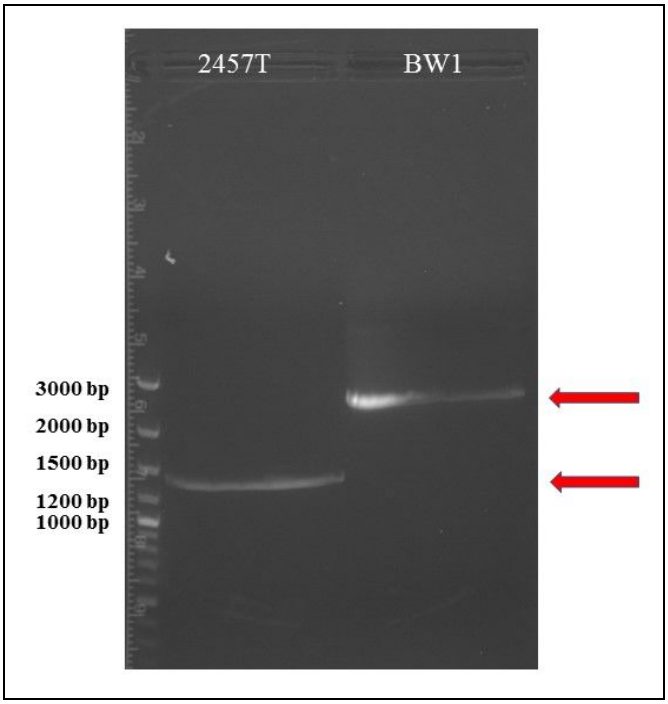

Figure 4. *Mutant BW1 Confirmation*. Following the confirmation PCR, products were analyzed on a 1% agarose gel and stained with ethidium bromide. Relative to WT bacteria (WT; lane 2), the product size increased for BW1 (lane 3) to confirm the transposon insertion site. Mutants BW7 and BW14 were also confirmed with this procedure (data not shown). Lane 1 contains a 100 bp plus ladder (ThermoFisher™).

Construction of Mutant Strains

PCR was used to amplify a chloramphenicol resistance cassette gene from pKD3 with 5' and 3' overhangs identical to the 5' and 3' regions of *waaG* and *waaJ* (**Table 2**). Recombinants were selected on chloramphenicol plates (5 μg/mL) and confirmed with PCR using confirmation primers (**Table 2**) that annealed to specific regions upstream and downstream of each gene to detect size difference caused by insertion of the chloramphenicol cassette (**Figure 5**; [72]). The resulting Δ*waaG* and Δ*waaJ* mutants were subsequently used for LPS structure analysis, as well as bile salts growth and biofilm formation analyses relative to WT bacteria. In addition, the

Faherty laboratory had in possession a Δ*galU* mutant that was added to all assays and used to expand upon previous analyses performed by the lab [54].

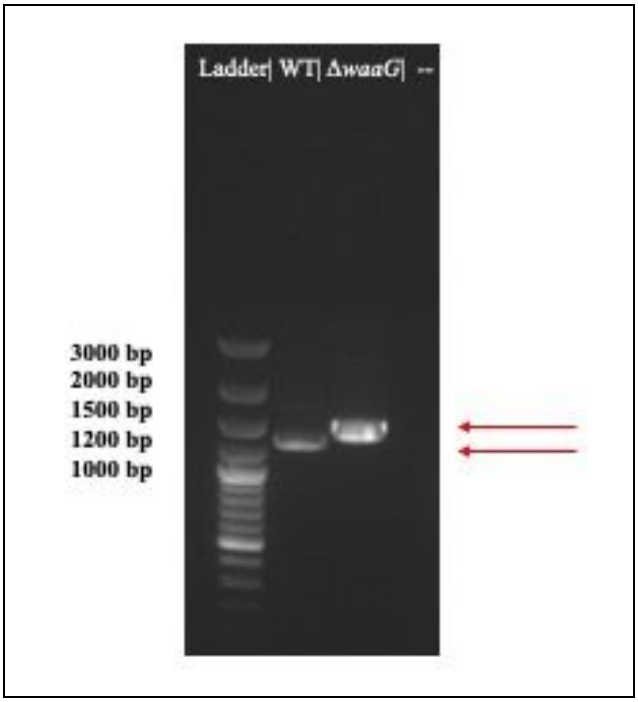

Figure 5. *Confirmation of LPS Core Biosynthesis Mutants.* An ethidium bromide stained 1% agarose gel showing confirmed Δ*waaG* gene deletion (Lane 3). Primers used are listed in Table 2. Lane 1 contains a 100 bp plus ladder (ThermoFisher™). Lane 2 contains the WT *S. flexneri*, and lane 4 is a no DNA template negative control reaction A size change was also detected for Δ*waaJ* (data not shown).

Purification and Visualization of LPS

The first analysis (**Figure 6**) evaluated the changes of the LPS structure purified from WT bacteria following growth in different media. Polyacrylamide gel electrophoresis was used to separate the LPS samples. Silver staining revealed that exposure to bile salts in both media types altered the Oag repeats. The WT Oag in LB (lane 2) can be seen from 37-65 kDa, while the Oag in TSB (lane 4) ranges from 35-70 kDa (white box). The Oag in LB + 0.4% bile salts (lane

3) does not extend as far, ranging from ~38-56 kDa (black box). In TSB + 0.4% bile salts (lane 5), the Oag ranges from 40 kDa to approximately 57 kDa (black box). Exposure to bile salts reduced the number of WT Oag repeat units as well as the range. Wild type LB had an average of 11.6 repeat units, while WT LB + 0.4% bile salts only had an average of 3.4 (**Table 4**). WT TSB (lane 4) had an average of 9.6 repeat units, while WT TSB + 0.4% BS had an average of 7 repeat units (**Table 4**). The WT TSB lane also had three distinct bands that are not present in the other lanes. There is a yellow band at 37 kDa (**Figure 6***,* boxed), hypothesized to be the first Oag repeat unit, 25 kDa (**Figure 6**, asterisk) and another yellow band at 15 kDa (**Figure 6**, star). The identities of these residues are waiting mass spectrophotometry results.

Finally, the lipid A, inner core, and outer core segments were detected in the region between 10 and 15 kDa (**Figure 6**, numbered 1-3; **Table 5**). Literature often refers to these residues as the lipid A and core component without further differentiating the bands. It is hypothesized based on the LPS structure (**Figure 2**), that lipid A falls at band number 3, the inner core is band 2, and the outer core is band 1. Following this hypothesis for WT LB, lipid A corresponded to a red band at 10 kDa, the inner core appeared as a yellow band found at approximately 12 kDa, and the outer core blue band resolved around 14 kDa. The three bands were at the same location in LB and TSB, but the bands were more intense in TSB. In LB + 0.4% bile salts, the lipid A component (lane 2, labeled 3) was fainter. The inner (2) and outer (1) cores shifted down in LB + 0.4% bile salts. The outer core was also fainter in LB + bile salts compared to LB. In TSB + 0.4% bile salts (lane 5), the outer core shifted down compared to TSB (lane 4). Overall, there was a reduction in band intensity in bile salts media compared to LB and TSB lanes. Also, the bile salts-treated LPS stained lighter compared to LB and TSB. Key WT

Oag bands, as well as lipid A, inner and outer core bands were excised from the gel and processed for mass spectrometry analyses, which are currently on-going at the time of writing this thesis. Future mass spectrophotometry analyses will include the marked mutant bands for Δ*galU,* Δ*waaG* and Δ*waaJ* (see below).

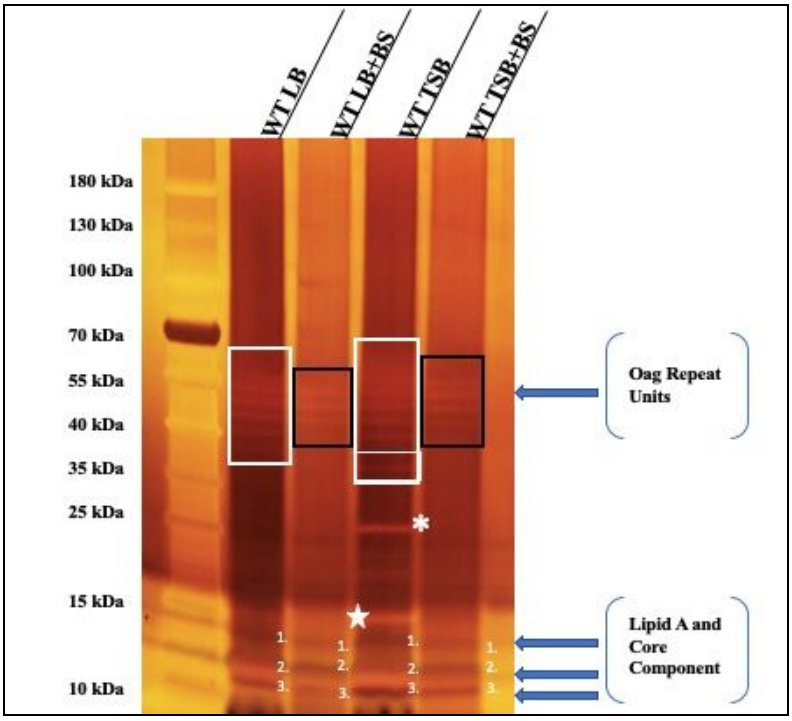

Figure 6. *Wild Type LPS in Various Media.* A 4-20% Tris-Glycine gradient gel (Criterion™) was used to visualize LPS structures following the hot aqueous-phenol extraction method to purify the structures as previously described (Davis & Goldberg, JoVE, [12]). The gel was loaded with 5 µL ladder and 6.55 µL LPS samples. Following electrophoresis, the gel was stained with a Colorimetric Silver Stain Kit (Pierce™). Lane 1, Ladder. Lane 2, WT LB, had 11 Oag repeat units from 37-65 kDa (white box). Lane 3, WT LB + 0.4% bile salts had 5 repeat Oag units from 38-56 kDa. Lane 4, WT TSB, had 7 Oag repeat units from 35-70 kDa, as well as 3 other unique bands: one orange band at 37 kDa (boxed), a yellow band at 26 kDa (asterisk), and a yellow band at 15 kDa (star). Lane 5, WT TSB + 0.4% bile salts had 5 repeat Oag units from 40-57 kDa. Outer core, inner core, and lipid A bands are noted in each lane as 1, 2, and 3, respectively. Key Oag, inner and outer core, and lipid A bands have been digested in trypsin and are waiting mass spectrophotometry analysis.

The second set of analyses evaluated the Δ*galU* mutant (**Figure 7**), which is unable to add the first glucose residue to the outer core [63]. Thus, the LPS of this mutant should only consist of lipid A and the inner core. The Δ*galU* mutant had the least amount of bands across all media types; significant residues are boxed or labeled. The Δ*galU* mutant in LB (**Figure 7,** lane 7) had two significant bands at 15 kDa and 20 kDa (boxed in green, labeled A and C respectively), as well as the bands hypothesized to be inner core (2) and lipid A (3) at 10 and 12 kDa, respectively. The Δ*galU* LB lipid A and inner core residues were less intense or not clearly defined as in WT LB (**Figure 6,** lane 2). Furthermore, the lipid A and inner core stained a different color (blue) in Δ*galU*, as opposed to red bands in WT (**Figure 7**, labeled 3), suggesting a molecular weight or charge residue modification. The Δ*galU* LB + 0.4% bile salts lanes had only one significant band at approximately 17 kDa (boxed in green, C), compared to WT LB + 0.4% bile salts (**Figure 6** lane 2) , as well as Δ*galU* in LB (**Figure 7** lane 7).

The Δ*galU* mutant in TSB had three significant bands between 15 and 20 kDa (**Figure 7**, lane 9, A, B, C). This lane was the only media type in which Δ*galU* expressed all three of these residues. Furthermore, Δ*galU* in TSB had 3 key bands between 10 and 15 kDa, similar to WT TSB, but with much less intensity. The lipid A component appeared light pink compared to the maroon band in WT (lanes 4 and 9, labeled 3), again suggesting a weight or charge residue modification. Surprisingly, Δ*galU* in TSB also seemed to have a very faint band that was in line with the hypothesized outer core of WT (lane 9, labeled 1).

Regarding the presence of additional bands in the Δ*galU* mutant, TSB + 0.4% bile salts (lane 10) had two key bands at approximately 16 kDa and 18 kDa (C. and B. respectively). These two bands were also present in Δ*galU* TSB, but were more orange in TSB + 0.4% bile salts,

compared to the lighter yellow bands seen in TSB. Δ*galU* in TSB + bile salts had the same three bands between 10 and 15 kDa as WT TSB + 0.4% bile salts and Δ*galU* TSB, with some modifications (**Table 5**). The outer core (band 1) in lane 10 was darker than the corresponding band in Δ*galU* TSB (lane 9) and lighter than the corresponding band in WT TSB + 0.4% bile salts (lane 5). Band 2, hypothesized to be the inner core, appeared in the same location as the blue band in WT TSB bile salts and the yellow band in Δ*galU* TSB, but the band was a more intense yellow. Band 3 in Δ*galU* TSB + 0.4% bile salts was less intense, lighter, and shifted about 1 kB up compared to the band in Δ*galU* TSB. Lastly, there appeared to be some faint Oag repeat bands in Δ*galU* TSB + 0.4% bile salts, which was surprising since the Δ*galU* mutation results in a full Oag deletion. Average Oag repeat units for Δ*galU* are reported in **Table 4**, while average locations of lipid A, inner core, and outer core are reported in **Table 5**. Future analysis will use mass spectrophotometry to determine the identities of specific residues for all Δ*galU* labeled bands.

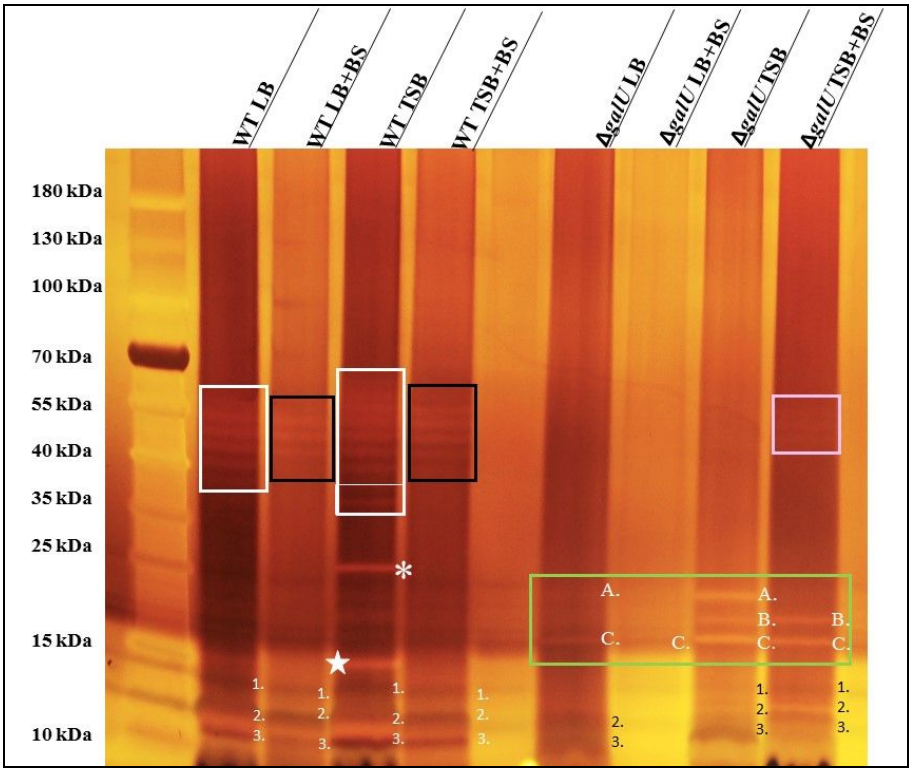

Figure 7. *WT and* Δ*galU Mutant Comparison in Various Media.* This figure expands upon the same gel and methods as Figure 6. Lane 1, Ladder. Lanes 2-5 are the same as Figure 6. Lane 6, no sample added. Distinct Δ*galU* bands of unknown composition are boxed in green and distinguished by A, B, and C. Lane 7, Δ*galU* LB had an orange band around 15 kDa (C), as well as a faint band at 17 kDa (A). Lane 8, Δ*galU* LB + BS had one faint band at 15 kDa (C). Δ*galU* TSB (lane 9) was the only mutant sample that had all 6 labeled bands from 10-20 kDa. Lane 10, Δ*galU* TSB + BS had two orange bands at 15 kDa (C) and 17 kDa (B), (same as the 2 bands in lane 9, but more orange compared to more yellow in TSB, suggesting a molecular weight or charge residue modification induced by bile salts media). The pink box in lane 10 represents a faint banding pattern that resembles the Oag repeat bands in WT TSB + 0.4% bile salts. The lipid A (3), inner core (2), and outer core (1) bands are labeled whenever detected for Δ*galU*.

The third silver stain analysis focused on the LPS core biosynthesis mutants, Δ*waaG* and Δ*waaJ* (**Figure 8**). In general, the Δ*waaG* and Δ*waaJ* mutants had less Oag repeat units relative to WT, but more than the Δ*galU* mutant across all media types (**Table 4, Figure 8**). The Δ*waaG* LB (lane 5) Oag repeat units (white box) ranged from 35-55 kDa, and Δ*waaG* LB + 0.4% bile salts Oag units (lane 6, black box) also ranged from 35-55 kDa. Both Δ*waaG* LB and LB + 0.4%

bile salts had a large brown/orange band ~12-15 kDa, but this band was thicker in Δ*waaG* LB. This band was predicted to be the lipid A and core for this mutant (**Figure 8,** blue box). The Δ*waaG* TSB (lane 11) Oag repeats were distributed from approximately 25-50 kDa (white box). This lane had the same brown/orange band ~13-15 kDa hypothesized to be the lipid A and core. The Δ*waaG* mutant in TSB + 0.4% bile salts consistently did not have LPS purified; and thus, the sample is not present in the gel. Average number of Oag repeat units for Δ*waaG* can be seen in **Table 4**, while average locations of lipid A, inner core, and outer core can be seen in **Table 5** (below).

Δ*waaJ* LB (lane 7), had Oag repeat units from 35-50 kDa (white box). Δ*waaJ* LB + 0.4% bile salts (lane 8, black box) had Oag repeat units from 35-55, same as Δ*waaG* LB + 0.4% bile salts. Both Δ*waaJ* LB and Δ*waaJ* LB + 0.4% bile salts had a brown/orange band at ~12-15 kDa like the Δ*waaG* mutant, but this band was thicker in Δ*waaJ* LB. Δ*waaJ* TSB (lane 12) had Oag repeat units from 25-45 kDa, while Δ*waaJ* TSB + 0.4% bile salts (lane 13) had no discernable Oag repeats. However, Oag repeats for Δ*waaJ* TSB + 0.4% bile salts were observed in one 4-20% Tris-Glycine gel (Criterion™) using the non-colorimetric and more traditional Pierce Silver Stain kit™, with 6 repeating Oag units from 35-55 kDa (data not shown). Δ*waaJ* TSB had a thick brown/orange band at ~12-15 kDa, thought to be the lipid A and core. Interestingly, Δ*waaJ* TSB + 0.4% bile salts had a faint brown/orange band around 13 kDa, which could represent just the lipid A component. Furthermore, the entirety of the Δ*waaJ* TSB + 0.4% bile salts lane had a lighter stain than the Δ*waaJ* mutant in any other media types. Compared to WT, both Δ*waa* mutants had shifted lipid A and core residues (**Figure 8, Table 5**). Both Δ*waa* mutations were expected to result in a partial or mostly complete outer core (Δ*waaG* and Δ*waaJ*,

respectively). The gel analyses did not result in significant separation of the lipid A and core components to be able to evaluate the three structures as was performed for the WT samples. Average Oag repeat units for Δ*waaJ* can be seen in **Table 4**, while average locations of lipid A, inner core, and outer core can be seen in **Table 5**.

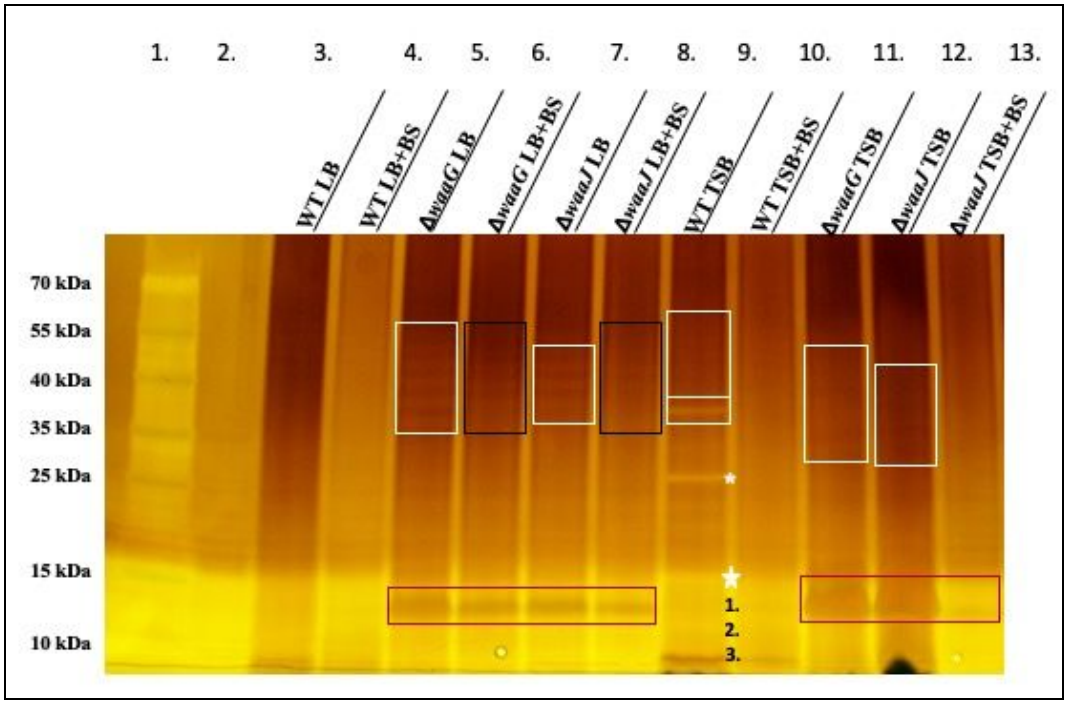

Figure 8. *WT,* Δ*waaG,* and Δ*waaJ Mutant Comparison in Various Media.*
The same procedure was used as described in Figures 6 and 7. Lane 1, Ladder. Lanes 3, 4, 9, 10 are the WT 2457T comparison as noted above. For reference, the LPS features for WT in TSB are noted as described in Figure 6. The Δ*waaG* LB Oag repeats (lane 5) are between 35 and 55 kDa, which is the same as Δ*waaG* LB + BS. Δ*waaJ* LB Oag repeats (lane 7) run from 35 to 50 kDa, while Δ*waaJ* LB + BS units run from 35-55 kDa. Δ*waaG* TSB Oag repeats (lane 11) run between 25 and 50 kDa, while Δ*waaJ* TSB Oag repeats (lane 12) run from 25 to 45 kDa. Δ*waaJ* TSB + BS (lane 13) does not have visible Oag repeats. Δ*waaG* TSB + BS did not have a sufficient number of bacteria for the LPS purification. One key band boxed in red is likely the lipid A and core components that are seen at ~12-15 kDa for all Δ*waa* lanes and shifted relative to WT. White boxes denote Δ*waa* Oag repeat units in LB and TSB, while black boxes denote Δ*waa* Oag repeat units in bile salts media.

Table 4. *Average Number of Oag Repeat Units per Media Type*. (n=3)

Strain	**LB**	**LB+ 0.4% BS**	**TSB**	**TSB+ 0.4% BS**
WT	11.6	3.4	9.6	7
Δ*galU*	0.75	0	0.75	2.75
Δ*waaG*	8.5	8.3	8	Not applicable
Δ*waaJ*	5	8	4.5	*6

*Asterisks indicate result detected in only one of the three gels.

Table 5. *Average Lipid A and Core Component Location per Media Type (color)* (n=3)

Strain	**LB**	**LB+ 0.4% BS**	**TSB**	**TSB+ 0.4% BS**
WT				
LipidA	7 kDa (maroon)	9-10 kDa (orange, maroon)	~8-9 kDa (orange)	9 kDa (thin orange, maroon)
Inner Core	10 kDa (one orange, one maroon)	12 kDa (brown)	~10-11 kDa (yellow, maroon, orange)	10 kDa (orange)
Outer Core	13 kDa (one yellow, one orange)	14 kDa (thick yellow)	15 kDa (thick yellow)	11 kDa (brown)
Δ*galU*				
LipidA	9 kDa (brown)	*10 kDa (blue)	7-10 kDa (light brown)	*10 kDa (blue)
Inner Core	13 kDa (orange)	15 kDa (blue)	11 (brown)	12 kDa (thick, orange)
Outer Core	*17 kDa (orange)	Not detected	*15 kDa (thick red/orange)	15 kDa (orange/red)
Δ*waaG*				
LipidA	12-15 kDa (brown/orange)	13-15 kDa (brown/orange),	13-15 kDa (brown/orange)	Not applicable
Inner Core	12-15 kDa	13-15 kDa	13-15 kDa	Not applicable

	(brown/orange),	(brown/orange)	(brown/orange)	
Outer Core	12-15 kDa (brown/orange)	13-15 kDa (brown/orange)	13-15 kDa (brown/orange)	Not applicable
ΔwaaJ				
LipidA	13-15 kDa (brown/orange)	13-15 kDa (brown/orange)	12-15 kDa (brown/orange)	12-13 kDa (faint brown/orange)
Inner Core	13-15 kDa (brown/orange)	13-15 kDa (brown/orange)	12-15 kDa (brown/orange)	12-13 kDa (faint brown/orange
Outer Core	13-15 kDa (brown/orange)	13-15 kDa (brown/orange)	12-15 kDa (brown/orange)	12-13 kDa (faint brown/orange)

*Asterisks indicate the results were detected in only one of the three gels.

Growth Curve Assay

In order to determine growth of LPS deletion mutants in bile salts, all bacteria were grown in TSB and LB media in the absence and presence of 0.4% bile salts following a 1:1 dilution from overnight growth (**Figures 9, 10, 11**). Interestingly, even though the growth conditions of the mutants were not significantly different from WT in TSB and LB (aside from *waaJ* at hour 8 and hour 12 in TSB; $p < 0.046$), the growth patterns in bile salts media had marked differences from the WT.

In TSB + 0.4% bile salts media (**Figure 9**), all strains experienced a decline in optical density upon bile salts exposure. The WT strain had an insignificant lag period of less than 1 hour before resuming normal growth, and it reached a maximum OD_{600} reading of 1.437 at hour 4. Δ*galU,* Δ*waaG,* and Δ*waaJ* all had significant periods of cell death as indicated by sharp decreases in the OD_{600} readings before recovering. On average: Δ*waaJ* returned to the initial OD_{600} reading after 12 hours, Δ*galU* at 8.5 hours, and Δ*waaG* never reached the initial OD_{600}

reading despite growing slowly over the 24 hour period. Statistical significance was calculated using a two-way ANOVA test. Results are as follows:

The Δ*galU* mutant optical density readings in TSB + 0.4% bile salts were significantly lower than WT during hours two ($p = 0.0075$), three ($p = 0.0067$), four ($p = 00.0081$), and five ($p = 0.0201$). After the fifth hour, growth of the Δ*galU* mutant was no longer statistically lower than WT, although the mutant did not reach WT growth until after 12 hours. Δ*galU* was the only mutant that reached WT optical density readings in TSB + 0.4% bile salts. The maximum OD_{600} value was 1.333 at hour 16.

The Δ*waaJ* mutant had significantly lower growth in TSB + 0.4% bile salts compared to WT at hour one ($p = 0.0139$), two, three, four, five, six, seven, eight, and nine, and ten (all $p \leq 0.0088$). This mutant did not reach WT levels of growth during the 24 hour period, though the difference in optical density was not statistically significant after hour ten. The Δ*waaJ* maximum OD_{600} reading in TSB + 0.4% bile salts was 1.088 at hour 14.

Finally, the Δ*waaG* mutant did not recover the original OD_{600} value within 24 hours, showing a bacteriostatic response in TSB + 0.4% bile salts. Though Δ*waaG* was not killed by the bile salts exposure, the mutant was unable to proliferate in TSB + 0.04% bile salts. The Δ*waaG* mutant did not reach WT growth; and thus, had significantly different growth in TSB + 0.4% bile salts compared to WT during hours 1-24 with the following significance: hour 1 had a p value of 0.0037, hours 2-11 ($p \leq 0.0001$) had the greatest difference, and hours 12-24 had p values $\leq$ 0.0371. The maximum OD_{600} reading for Δ*waaG* in TSB + 0.4% bile salts was 0.940 at hour 22.

During LB + 0.4% bile salts exposure (**Figure 10**), all mutants had a period of decline in optical density readings. The WT strain had an insignificant lag period of less than 1 hour before resuming normal growth. Δ*galU* recovered to the initial OD_{600} value after hour 5, Δ*waaG* recovered to the initial OD_{600} value after hour 4, and Δ*waaJ* recovered to the initial OD_{600} value after hour 9. Wild type had a maximum OD_{600} value of 1.640 at hour 4 before entering the static phase. Statistical significance was calculated using a two-way ANOVA test and the results are as follows:

The Δ*galU* optical density readings in LB + 0.4% BS were significantly lower than WT during hours 1-10. Hour one had a p value of 0.0012, hours 2-7 had a p value ≤ 0.0001, and hours 8-10 had a p value ≤ 0.0343. After hour 11, Δ*galU* was no longer statistically different from WT, but it did not reach WT levels in LB + 0.4% bile salts until hour 16. Δ*galU* had a maximum OD_{600} value of 1.459 at hour 24 in LB + 0.4% bile salts.

The Δ*waaJ* mutant had significantly lower growth than WT in LB + 0.4% BS between hour 0 and hour 10. Hour 0 had a p value of 0.0011, and hour 10 had a p value of 0.0320. Hours 1-9 all had the same value: $p \leq 0.0001$. Δ*waaJ* did not reach WT growth in LB + 0.4% BS, but the difference in growth was not significant after hour 10. Δ*waaJ* reached its maximum OD_{600} reading of 1.356 at hour 15.

Surprisingly and unlike growth in TSB + 0.4% bile salts, the Δ*waaG* mutant recovered to the initial OD_{600} reading at hour 3 in LB + 0.4% bile salts. Δ*waaG* was significantly lower from WT in LB + 0.4% BS during hours 1-8. Hour 1 had a p value of 0.0052, hours 2-4 had a p value <0.001, and hours 5-8 had a p value ≤ 0.0188. Δ*waaG* did not reach WT levels of growth, but

differences were not significant after hour 8. The maximum optical density for Δ*waaG* was 1.38 at hour 14.

In all, the three mutants had significantly lower growth in both media types with bile salts compared to WT. Δ*galU* was the only mutant to reach WT optical density readings, which occurred at hour 12 in TSB + 0.4% BS and hour 16 in LB + 0.4% BS. In TSB + 0.4% bile salts, both Δ*galU* and Δ*waaJ* recovered to the initial optical density readings, at 8.5 and 12 hours, respectively, while Δ*waaG* was unable to do so. Interestingly, Δ*waaG* reached the original OD_{600} reading at hour 3 in LB + 0.4% bile salts, marking a very brief period of cell death. Δ*galU* reached the initial optical density reading at hour 5 in LB + 0.4% bile salts. Finally, Δ*waaJ* recovered to the initial optical density reading at hour 9.

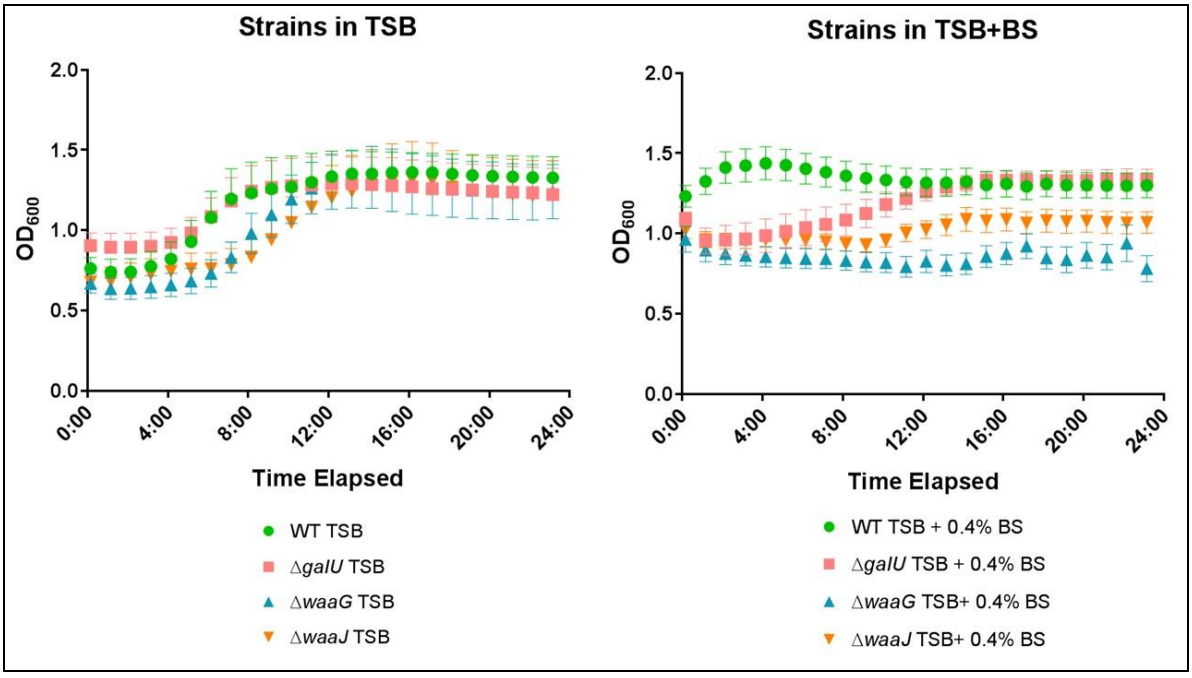

Figure 9. *Comparison of Growth in TSB and TSB + Bile Salts Media.* All strains were grown overnight in 10 mL TSB at 37℃, then resuspended in 10 mL TSB +/- 0.4% bile salts. OD_{600} readings were taken every 10 minutes for 24 hours using an Epoch 2 microplate reader (BioTek™). GraphPad Prism software was used for graphical representation. Data represent the

average of 3 experiments, each with 3-5 technical replicates for bile salts media; and 2 experiments with 3-5 technical replicates for TSB. Statistical analyses were performed using an ANOVA analysis. The error bars represent the standard error of the mean (SEM). Any data point in which the SEM bars do not overlap with WT were significantly different for each mutant (see text for details). Results show that the Δ*galU* mutant was the only mutant to reach WT levels of growth in bile salts media. Δ*waaJ* in bile salts did not reach WT growth levels, but did reach its initial OD_{600} reading at 12 hours. Δ*waaG* had a bacteriostatic response in bile salts as it never reached its initial OD_{600} reading.

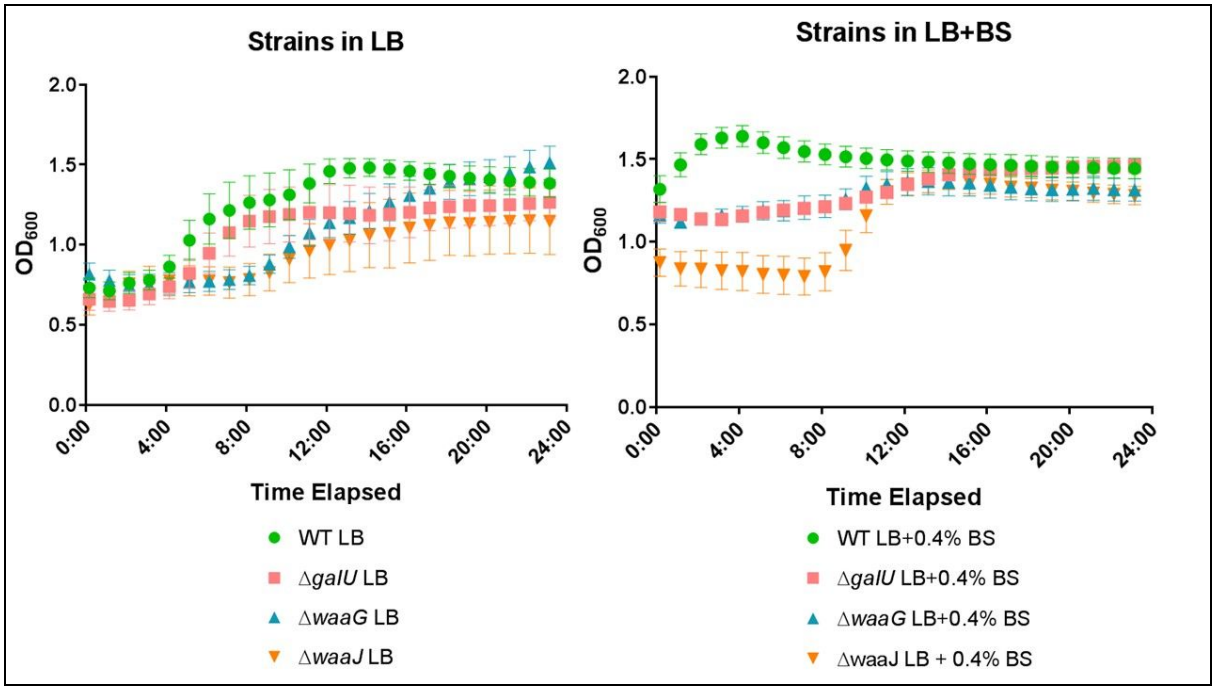

Figure 10. *Comparison of Growth in LB and LB + Bile Salts Media.* All strains were grown overnight in 10 mL LB at 37℃, then resuspended in 10 mL LB +/- 0.4% bile salts. Growth was recorded and plotted as described above with the same biological and technical replicates. The mutants had slower growth in bile salts media compared to WT. Δ*galU* reached WT growth levels after 16 hours, but the Δ*waaJ* and Δ*waaG* mutants did not reach WT growth. The same statistical analyses were performed as described above.

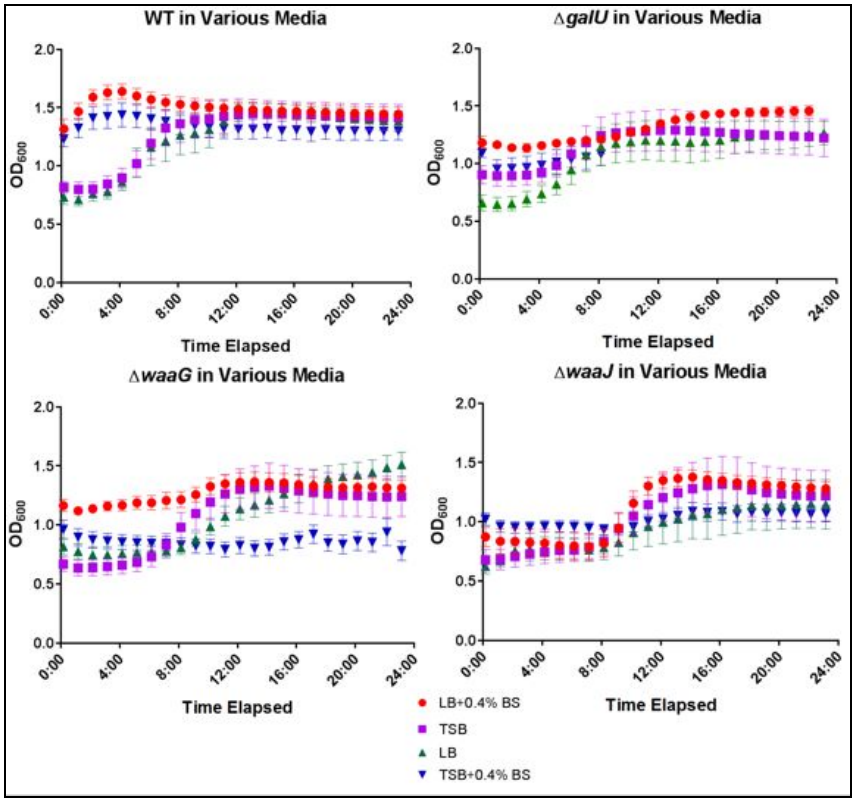

Figure 11. *Comparison of Growth by Strain in Various Media*. All strains were grown overnight in 10 mL TSB or LB at 37℃, then resuspended in 10 mL TSB or LB +/- 0.4% bile salts. Growth was recorded and plotted as described above with the same biological and technical replicates. Results show that Δ*galU,* Δ*waaG* and Δ*waaJ* mutants have a period of cell death following bile salts exposure not seen in TSB and LB or in WT with bile salts exposure. On average, all strains had more higher readings in LB + 0.4% BS compared to TSB + 0.4% BS.

Biofilm Solid-Phase Adherence Assay

Because *S. flexneri* has been found to form a biofilm in response to bile salts exposure and is a proposed mechanism for the pathogen to survive intestinal transit [54], the abilities of LPS mutants to form a biofilm were compared to WT (**Figure 12**). All bacteria were grown in TSB in the presence of 0.4% bile salts since both glucose and bile salts are required for biofilm formation [54 55]. Wild type in TSB was used as the negative control, and WT biofilm formation in bile salts served as the positive control. The WT cultures released a white precipitate typical of

EPS matrix production and visible bacterial aggregates in the presence of bile salts, both of which are indicative of biofilm formation. All three mutants had a significant reduction or were unable to form a biofilm in response to bile salts in both a 1:50 dilution and a 1:1 dilution (**Figure 12** and data not shown, respectively). In comparison to WT in TSB, the WT in bile salts had statistically significant biofilm formation ($p < 0.0001$), as did the Δ*galU* TSB + 0.4% bile salts ($p = 0.0012$) (**Figure 12**). Though the Δ*galU* mutant displayed some adherence phenotype as measured by the OD_{540} reading, the mutant did not release EPS in the biofilm assay and did not resemble WT in the presence of bile salts. The Δ*waaG* and Δ*waaJ* mutants had a lower optical density reading in bile salts than WT in TSB, indicating a complete lack of adherence and biofilm phenotypes. LB and LB + 0.4% bile salts were not tested in this analysis, since it has been shown that both sugar and bile salts are required for biofilm formation [53 54].

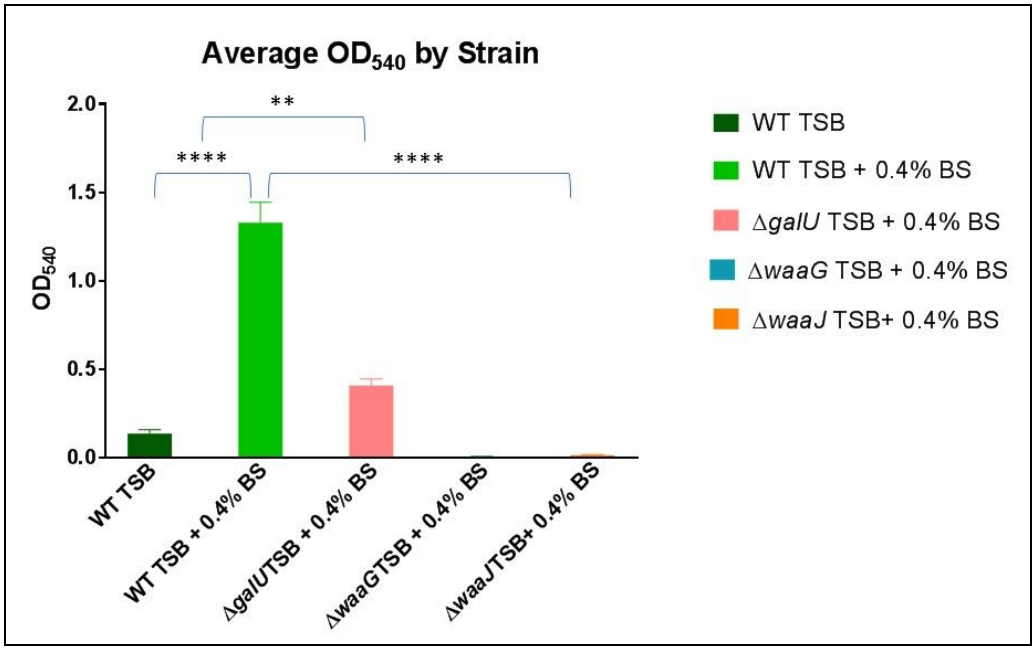

Figure 12. *Biofilm Formation Analysis of the LPS Mutants vs WT.* Average OD_{540} values between two biological replicates and 11 technical replicates of a slightly modified biofilm assay (Nickerson; JoVE).Wild type TSB was used as a negative control media since biofilm formation

requires bile salts. TSB + 0.4% bile salts were used in all other experimental wells. A two-way ANOVA test was used to compute the statistical significance. Statistical significance is noted using asterisks in which **** represent p value < 0.0001 and ** represent p = 0.0012. All mutants were tested against WT in TSB+BS. Interestingly, the Δ*galU* mutant had some biofilm formation while both Δ*waa* mutants failed to produce a biofilm.

Discussion

Diarrheal disease causes one in ten child deaths during the first five years of life, especially in communities lacking proper sanitation, facing undernutrition, and/or having high HIV burdens. *Shigella* is one of the top four pathogens in sub-Saharan Africa and South Asia [33], causing severe pediatric morbidity that is exacerbated in immunocompromised or malnourished children who often suffer from wasting or growth stunting [34]. Unfortunately, contracting dysentery only increases the nutritional deficiencies in these children. In settings without proper hygiene and sanitation, *Shigella* infections spread faster and cause increased morbidity and mortality, revealing the importance of proper sanitation techniques.

Due to the global infection rates and the emergence of multidrug resistant strains, there is a need to find appropriate vaccine targets for multiple *Shigella* serotypes. Because *Shigella* has 50 serotypes, a vaccine attempting to include LPS as a target must elicit immune responses against multiple Oag configurations. Live oral vaccines and Oag-polysaccharide conjugated vaccines have yielded promising protection data against a few *Shigella* serotypes, but no broad *Shigella* vaccine has ever been successfully developed [41]. *Shigella* vaccine development has not considered the effects of bile salts exposure on LPS, which could alter antigen targets relative to LPS isolated from bacteria grown in standard laboratory media. Thus, this research aimed to identify how the *S. flexneri* LPS is modified in response to bile salts exposure. Our research

suggests that *Shigella* can modify the LPS structure to evade the bactericidal effects of bile salts. The long term goal of this work is to identify the specific bile salt-induced LPS alterations and to determine if these alterations can be incorporated in vaccine formulations that would ultimately prevent *Shigella* infections.

Transposon Mutant Analysis

The *S. flexneri* genome is annotated with multiple genes of unknown function, as well as hypothetical proteins. *S. flexneri* also lacks annotation to regions predicted to encode genes. In order to complement previous RNA-sequencing data [54 65] and help identify genes essential for bile salts resistance and biofilm formation, a transposon library was created. This library consisted of 1,137 mutants that were screened for phenotypic defects that focused both on the ability to survive in bile salts and the ability to form a bile salt-induced biofilm. These qualifications narrowed down 37 mutants that exhibited abnormal behavior in bile salts. The RATE and confirmation PCR procedures were then used to identify the genes disrupted by each transposon insertion event in each mutant.

Mutants 1, 3, 4, 7, 10, 14, and 21 had slow or no growth in bile salts compared to WT. The predicted disrupted genes of each mutant were annotated to be involved in outer membrane structure, sugar transport, or LPS biosynthesis according to analyses using the Universal Protein (UniProt [68]) Resource database (Uniprot [68]). Mutant 7, *malM*, encodes a periplasmic protein hypothesized to be a part of the outer membrane. Mutants 3 and 4 mapped to the same gene, *mdtQ*, which encodes a multidrug resistance outer membrane protein that has drug efflux activity to remove toxic chemicals from the bacterial cell. Mutant 10, *yidjE*, is predicted to encode a transporter in the major facilitator superfamily (MFS) family of efflux pumps. Efflux pumps

consist of transporter proteins that aid in resistance to stressful conditions, such as antibiotics and bile salts [56]. Mutant 14 disrupted a gene named *ydjI* that is a fructose-bisphosphate aldolase and likely plays a role in zinc ion binding and chemical reactions involving carbohydrates.

Mutant 1 also had slow growth in bile salts as found by the Faherty lab. The transposon insertion was mapped to disrupt insertion sequences S4097 and S4098 (**Figure 2**). This region is between the *kdta* and *waaQ* LPS biosynthesis genes; and thus, the EZ-Tn5 likely affects the promoter regions of one or both of the genes. The *waaQ* gene encodes an LPS core biosynthesis protein that transfers glycosyl groups (Uniprot [68]). Disruption of *waaQ* would result in a LPS structure very close to the *galU* deletion since both remove nearly the entire outer core and Oag. The Tn5 insertion in BW1 is also close to *kdta*, or *waaA* at locus S4096, which encodes 3-deoxy-D-manno-octulosonic acid transferase (Uniprot [68]) that attaches the lipid A to the core via the KDO residues (**Figure 2**). Because the genes disrupted by BW1 are in opposite orientation, both promoters and thus expression of both genes could be affected by the transposon insertion (**Figure 2**). In the future, RT-PCR can be used to determine if one or both of these genes are improperly transcribed in BW1. Preliminary analysis of BW1 by the Faherty lab found that the mutant had a rapid increase in OD_{600} at approximately 3.5 hours in TSB + 0.4% bile salts, suggesting that the mutant releases EPS matrix at this time. Compared to WT, the mutant grew slower in bile salts, as WT releases its EPS matrix about an hour earlier. The mutant did not grow sufficiently in LB or LB + 0.4% bile salts, so the added glucose in TSB facilitates growth. Indeed, the availability of sugars in the small intestine [28] will be important considerations when evaluating the growth of these mutants in the presence of bile salts.

Finally, BW21 likely has a disruption in the gene *rfbG,* which encodes the protein dTDP-rhamnosyl transferase (Uniprot [68]). This protein is involved in transferring glycosyl groups during the lipopolysaccharide biosynthetic process. After confirming the identity of BW1, BW7, and BW14, mutant 1 had the most direct connection with LPS, although BW21 is still pending confirmation of the gene disruption. Preliminary results for BW21 by the Faherty lab showed that this mutant did not have a single, rapid increase in growth in TSB + 0.4% bile salts, but rather steadily increased beginning at 5 hours. This growth pattern is not necessarily indicative of the bacteria releasing EPS, although further experimentation is needed to determine the effects of the mutation on growth and biofilm formation in the presence of bile salts. The mutant did not have an increased optical density reading in LB + 0.4% bile salts; and thus, it likely needs additional sugar to proliferate in bile salts media, which again correlates with the sugar availability in the small intestines [28].

Both BW1 and BW21 thus far had slow growth in all media types compared to wild type, suggesting that *waaA/kdta* or *waaQ* and *rfbG* genes play a role in bacterial growth. Preliminary analyses also suggest that at least one mutant was capable of forming a biofilm. Further experimentation will confirm these results and evaluate the LPS structure of the mutants.

Construction of Mutant Strains

Considering the points outlined above and the known literature of bile salt-induced LPS alterations in other pathogens highlighted in the introduction [23 31 46 54 63], the central focus of this thesis shifted to creating and analyzing LPS mutants with distinct truncations. Therefore, deletion mutants of *waaG* and *waaJ* genes were constructed to be evaluated with the Δ*galU*

mutant already in possession in the Faherty Lab. Because LPS core biosynthesis mutants have been shown to be immunodeficient in *Salmonella, Vibrio,* and *E. coli* [31] [51] [53] and the gene mutations have generated easily visualized LPS truncations in other studies [43], the *waa* genes were selected for further investigation. The Δ*galU* mutant was also used given the complete deletion of the outer core and Oag, as well as the previous analyses performed by the Faherty lab [54]. For the Δ*waa* mutations, the deletion protocol replaced each gene with a chloramphenicol resistance cassette [72]. The cassette contains three stop codons in each reading frame to prevent polar mutations. Furthermore, the mutants were constructed to leave the native start and stop codons for each *waa* gene. Therefore, we expect that each mutation is a single gene mutation and does not affect other genes in the operon (**Figure 2**). Future complementation analyses for each mutant should be performed to confirm the results. As needed, RT-PCR analysis of the downstream genes can confirm gene expression, and the chloramphenicol resistance cassettes can be removed [72] to prevent polar effects .

Considerations for Chosen Methodology

When first growing the mutants in bile salts media, especially for the LPS extraction, a standard laboratory technique using a 1:50 dilution from overnight cultures was used so the bacteria could efficiently reach mid-log phase of growth in the bile salts test media. With WT and Δ*galU*, this dilution produced a sufficient bacterial pellet after a longer incubation. However, with the Δ*waaG* and Δ*waaJ* mutants, this dilution did not produce a sufficient amount of bacteria in bile salts media. To account for the reduced growth and to obtain sufficient amount of bacteria for all analyses, an alternative strategy successfully produced a pellet: the mutants were cultured

for about 18 hours in 10 mL TSB or LB, centrifuged the next day for ten minutes at 4000 rpm, and pellets were resuspended 10 mL TSB or LB with 0.4% bile salts following one wash with 1X PBS. This extended incubation time, in combination with the 1:1 resuspension, resulted in appropriate bacterial growth for all mutants, aside from Δ*waaG* in TSB + 0.4% bile salts media that produced a bacteriostatic effect and correlated with a lack of LPS purification. The same 1:1 dilution strategy was used for growth with control media (TSB or LB without bile salts) to ensure consistency across all media types.

Future experiments should be performed to explore the effects of this resuspension method on the bile salts resistance abilities of each mutant. Additionally, 48 hour incubation times with a 1:50 dilution can be pursued to determine if the mutants can eventually compensate with longer incubation times. A consistent lack of growth with the 1:50 dilution would indicate that bile salts are either bactericidal or bacteriostatic for the mutants. Based on our analyses, it is likely the higher number of bacterial cells in the 1:1 resuspension, or a subpopulation following cell death, was able to tolerate the bile salts exposure and subsequently express compensatory mechanisms in order to grow. Indeed, identification of these mechanisms would provide valuable information toward our understanding of bile salts resistance in *S. flexneri*. We hypothesize that changes to outer membrane proteins or structures, including extensive adaptation to remaining LPS components, and/or higher expression of efflux pumps are possible compensation mechanisms [54 65]. As noted, the Δ*galU* mutant was able to grow in the 1:50 dilution after the longer incubation, which suggests a more efficient compensation mechanism relative to the Δ*waa* mutants. In fact, the data suggest that a partial or incomplete outer core is more detrimental to the bacteria compared to the absence of the outer core. One growth curve

experiment was performed using a 1:50 dilution for comparison (data not shown), revealing slower growth of the mutants relative to WT in all media types, in which none of the mutants reached WT levels. For both WT and the Δ*galU* mutant, the LPS purification and growth curve analyses should be performed with the 1:50 dilution to determine if the results are consistent with the 1:1 dilution method. In summary, WT, Δ*galU,* Δ*waaG,* and Δ*waaJ* were treated with this 1:1 dilution growth method in the experiments, aside from the standard procedure of the biofilm solid-phase adherence assay, to ensure the same treatment of all samples.

Purification and Visualization of LPS

The purification of LPS using the hot aqueous-phenol method isolates the LPS from any proteins and nucleic acids that obstruct LPS visualization. Following this extraction, the samples were analyzed using polyacrylamide gel electrophoresis (**Figures 6, 7, 8**). The Tris-Glycine 4-20% gradient gels (Criterion™ Dodeca™) showed separation of bands and uniformity of gels with a colorimetric silver stain (Pierce™). A second silver stain (Pierce™) with a reduced background paired with a Tris-Tricine 4-16% gel (Criterion™) was also used. The Tris-Glycine gels had the best results with the colorimetric silver stain, which stains the entire gel an amber color and shows distinctly colored bands based on varying concentration. Unfortunately, the amber color of the stain made it difficult to photograph the gels, hence additional observational data are provided and summarized in **Tables 4 and 5**. The Tris-Tricine gel with the silver stain did not have this amber background, leading to better visualization of key bands; however, there were less bands represented on the gel. Thus, the results are presented using the Tris-Glycine gel

with the Colorimetric Silver Stain, as these gels produced the most bands with clear distinction among each band.

For WT, bile salts exposure resulted in fewer Oag repeat units on average (**Table 4**). Furthermore, the size shift in the start of the Oag repeat (*e.g.* starting at 35 kDa in TSB vs. 40 kDa is TSB + 0.4% bile salts) suggests that each Oag repeat band had a heavier composition in bile salts. The mass spectrometry analyses will define the Oag modifications in bile salts and help to determine if additional experimentation is required to define these alterations following bile salts exposure. We hypothesize that these Oag changes are not due to delayed growth kinetics, but rather due to specific modifications to the Oag in the presence of bile salts, since growth was not significantly delayed relative to media without bile salts. The shorter Oag result is in contrast to the observations with *Salmonella* and bile salts in which longer Oag repeats aided the bile resistance strategies of the pathogen [31]. This pathogen comparison highlights that while enteric bacteria may use similar strategies to resist bile salts (*i.e.,* variation of Oag length), the specific changes may contrast (*i.e.,* shorter Oag in one pathogen vs. longer Oag in another pathogen). The shorter *S. flexneri* Oag in response to bile salts is supported by a recent examination of a Δ*tolR* mutant as a *S. flexneri* vaccine candidate [57]. The LPS isolated from outer membrane vesicles of the Δ*tolR* mutant displayed longer Oag chains relative to WT, and the mutant was sensitive to deoxycholate exposure. Therefore, shorter but likely modified Oag repeats appear to facilitate bile salts resistance in *S. flexneri*.

The WT samples exposed to bile salts also had additional modifications. The outer core band (1) was shifted down 1-2 kDa with a thinner and fainter band compared to TSB and LB, suggesting a modification in this region to allow for growth in bile salts. The inner core band (2)

was also thinner and shifted down 1-2 kDa in bile salts media (**Figure 6**). Furthermore, while the lipid A band remained at 10 kDa for all WT samples, the band (3) was dark maroon in LB and TSB and only faint pink in bile salts media, suggesting reduced expression of this residue in bile salts. As noted above, the core and lipid A modifications are likely due to bile salts exposure since growth is not significantly affected. Finally, the unique bands present in TSB are interesting and require identification, especially given the sugar availability in the small intestine [28]. The mass spectrometry data will confirm the results from the LPS extraction analyses. In all, the analyses performed here generated significant data toward our understanding LPS modifications in conditions that mimic the small intestinal environment. The ramifications of these changes on immune recognition certainly needs to be investigated.

The Δ*galU* mutant did not have as many bands as WT as expected, aside from the hypothesized lipid A and inner core bands from 7-10 kDa (**Table 5**). Because *galU* synthesizes UDP-glucose, the mutant is unable to add the first glucose residue to the outer core [63]; and thus, only lipid A and the inner core should be present. Between 15-25 kDa, the banding pattern was different relative to WT for all media types; and in addition, this banding pattern and concentration varied across media types for the Δ*galU* mutant. Mass spectrometry analysis will be vital to identify these bands and to determine what changes occur as a result of glucose and/or bile salts exposure.

Since the Δ*galU* mutant does not have an outer core and Oag, yet still grew better than the Δ*waa* mutants in bile salts, the data suggest that the lipid A, inner core, and/or other noted band modifications (A-C) may have more of an impact on growth in bile salts. Interestingly, it appears a band similar to the outer core was visible in LB (n=1), TSB (n=1), and TSB + 0.4%

bile salts (n=4). Furthermore, an Oag appeared visible in TSB + 0.4% bile salts (once with a tris-glycine gradient gel (Criterion™ Dodeca™) as seen in **Figure 7** and once in a tris-tricine gradient gel (Criterion™; data not shown)). Analyses should be repeated since detection of most of these components were variable aside from the consistent appearance of the outer core in TSB + bile salts. Future mass spectrometry will confirm the identification of these bands to help us understand the LPS compensation mechanisms in these conditions. It is possible that *S. flexneri* uses another gene to compensate for a Δ*galU* mutation in the presence of glucose, in which this compensation is further enhanced in bile salts to enable the mutant to grow in the stressful conditions. Additional LPS related genes or possible UDP-glucose gene homologs need to be analyzed. Therefore and based on the analyses performed here, the Δ*galU* mutant could help us identify additional LPS-related genes that are important to understand how *S. flexneri* alters the LPS structure in the small intestinal environment in the presence of both glucose and bile salts.

The Δ*waa* mutants also had significant differences in the respective LPS structures. Interestingly, the lipid A and core residues were shifted higher compared to WT and ranged from 12-15 kDa (**Figure 8**). The bands were thick and brown/orange in the mutants across all media types with little to no noted distinctions as the media varied. Importantly, the lipid A and core residues did not separate into 3 distinct bands like the three thin maroon bands in WT. The data suggest that the lipid A and core residues were therefore modified in both Δ*waa* mutants. The lack of separation of each component likely explains the larger size. Each mutation results in either a partial (Δ*waaG*) or almost complete (Δ*waaJ*) outer core; but these differences were not discernable on the gel, especially with the lack of separation from the lipid A and inner core. Thus, further analysis is needed to determine how the remaining outer core components are

altered in the presence of glucose and/or bile salts. We also currently cannot rule out modifications to lipid A or the inner core without future mass spectrometry analyses.

Regarding the Oag repeat units, the Δ*waa* mutants had fewer Oag repeat units relative to WT in LB and TSB, but were nonetheless detected (**Figure 8, Table 4**). The mutations should have resulted in a lack of Oag production, but the results were consistent and seen across all media types. The results suggest that an LPS outer core truncation does not eliminate the full Oag. It will be interesting to determine if the Oag was simply attached to each incomplete outer core or if the mutants first compensated by using additional genes to complete the outer core prior to the attachment of the Oag repeats. Future analyses need to determine which strategy was used and which genes could compensate for the Δ*waa* mutations in order to both complete the outer core and/or add an Oag. Additionally, mass spectrometry will determine if each Oag repeat is modified relative to WT in the different media compositions.

It is likely that the outer core remains incomplete in each Δ*waa* mutation, especially due to the changes observed in the bile salts media. Interestingly, the Δ*waa* mutants had more Oag repeat units in LB + bile salts media compared to WT. The Δ*waaG* mutant did not reduce the number of Oag repeats while the Δ*waaJ* mutant increased the number (**Table 4**). These results could be a compensation for an incomplete outer core, and it will be interesting to determine if mass spectrometry can detect other modifications. Despite these changes in LB + bile salts media, the presence of glucose had a more significant impact on the LPS structure in bile salts for the Δ*waa* mutants. The LPS could not be purified for Δ*waaG* in TSB + bile salts, which is likely due to the growth kinetics (see below). The Δ*waaJ* mutant had a faint band from 12-13 kDa representing the lipid A and core in the presence of TSB + 0.4% bile salts, and an Oag was

detected in only 1 gel upon repeated analysis. While Δ*waaJ* may be better at compensation and thus have a modified LPS structure in this media type compared to Δ*waaG*, these results indicate there is added stress on an incomplete outer core from the glucose in the presence bile salts. Neither mutant had the additional TSB modifications identified in WT as noted by the stars and asterisks in **Figures 6-8**, which again is likely a result of an incomplete outer core and therefore may impact the ability of the mutants to modify the LPS structure in the presence of bile salts. Future mass spectrophotometry analysis will help to understand the results, characterize each LPS component in the Δ*waa* mutants across all media types, and determine the importance of each modification in glucose, bile salts, or the combination.

Growth Curve Analyses

All bacteria were grown in TSB and LB in the absence and presence of 0.4% bile salts following a 1:1 dilution (**Figures 9, 10, 11**). Analyses with a standard 1:50 dilution should be performed, possibly with longer incubation times, which will be important to determine if bile salts are bacteriostatic or bactericidal for each mutant. Furthermore, the analyses would help with the overall mutant characterization since the Δ*galU* mutant was able to grow in bile salts with the 1:50 dilution while the Δ*waa* mutants were unable to grow. It is likely that a 1:50 dilution does not yield a sufficient amount of bacteria for the Δ*waa* mutants to survive bile salts exposure and express compensatory mechanisms for eventual growth. Furthermore, the Δ*waa* mutants were unable to grow if the bacterial colonies were not freshly restreaked (*i.e.* older than 1 week) on agar plates, even in the 1:1 dilution conditions. If older colonies were used, only WT and Δ*galU* grew, which indicates that the Δ*waa* gene deletions were stressful on the bacteria. Importantly,

the data clearly demonstrate that the Δ*galU* mutant was more efficient at compensating for bile salts growth compared to either of the Δ*waa* mutants. As noted above, partial or incomplete outer cores appear more unstable relative to complete loss of the outer core, which would impact the bacteria prior to any compensatory modifications used to facilitate bile salts resistance.

For the 1:1 dilution with fresh bacteria, all strains grew normally in TSB and LB, and any differences between mutants and WT were not statistically significant. For bile salts media, WT bacteria had an insignificant lagging period upon exposure to bile salts before continuing to grow as normal, whereas the mutants had growth delays of several hours following bile salts exposure. The data demonstrate that the mutants can compensate during this lagging period in order to properly initiate growth. Possible compensation mechanisms include alterations to the remaining LPS structures as discussed above for the LPS gel analyses, additional changes to the outer membrane including protein composition [65], and induction of multidrug efflux pumps [56 65]. Future experiments including characterization of the outer membrane proteins, expression analyses of the efflux pump genes, and further mutational analyses should be performed in conjunction with mass spectrometry of the LPS structures in order to define all compensation mechanisms. Some outer membrane protein changes have been detected in *S. flexneri* following bile salts exposure [14], but specific identification of the proteins remains to be determined.

Assuming the LPS structures are the predominant mechanisms of compensation for the eventual growth of each mutant in bile salts media, some interesting distinctions are noted. First, the Δ*galU* mutant was able to recover to the initial OD_{600} value in LB + 0.4% bile salts at hour 5 and at hour 8.5 in TSB + 0.4% bile salts. These results are consistent with previous results that depict the lack of Δ*galU* growth in the first 6 hours of bile salts exposure in TSB [54]. This growth

pattern suggests that Δ*galU* compensates for the bactericidal effects of bile salts by modifying some aspect of the LPS structure during this 5-8.5 hour time frame; and once the compensation is completed, the bacteria can grow sufficiently. Furthermore, despite the longer compensation time in TSB + 0.4% bile salts, the mutant was able to reach WT levels at a quicker rate when additional glucose was present. Indeed, the differences between bile salt growth compensation in the presence and absence of glucose certainly warrant future investigation.

Since the Δ*galU* mutant lacks both the outer core and Oag, it is possible that the lipid A and inner core residues have important roles in bile salts resistance. Modified lipid A and inner core components could account for the fact that Δ*galU* grows better than Δ*waaG* and Δ*waaJ*. Although Δ*galU* cannot add the first glucose residue to the outer core [63], the mutant could possess alternative pathways to form an outer core. In *Vibrio cholerae*, a mutation in *galU* creates a mutant that lacks glucose binding to the first heptose (Hep1) residue; however, an intact Oag was produced with an altered core oligosaccharide composition [53]. This result is similar to the data presented here with TSB + bile salts media. Mass spectrometry analysis will confirm any modifications, but the results indicate the Δ*galU* mutant can modify the LPS structure for appropriate growth in the presence of bile salts.

The Δ*waaG* and Δ*waaJ* mutants had similar (but not identical) growth patterns, which is unsurprising considering the similarities of the LPS structures (**Figure 2**). These mutants showed increased growth deficiencies in bile salts media compared to Δ*galU.* There are two likely reasons for the added growth delays. First, it is possible that the presence of an incomplete outer core in the Δ*waa* mutants is more unstable for *S. flexneri* compared to complete loss of the outer core in the Δ*galU* mutant. Another possibility is that the Δ*waa* mutants took longer to

compensate and grow since the mutants were using alternative strategies to generate a more complete LPS structures. Clearly, the Δ*waa* mutants have more Oag repeats than the Δ*galU* mutant; and therefore, the mutants were able to ultimately produce a more complete LPS structure to resist bile salts in which longer time would be needed for this compensatory mechanism. It is quite interesting to contemplate the genetic changes that occur during the extended growth delays that eventually enabled growth of the mutants. Certainly, these observations highlight the need for the mutants to survive and are worth considering for future therapeutic development. Additionally, it is important to highlight that both Δ*waa* mutants had different phenotypes in bile salts relative to WT and Δ*galU*. After incubating in bile salts, there were large, free floating aggregates of cells in the tubes that had a sticky texture. It is likely that these cell aggregates were lysed cells, considering these observations were not seen in the WT and Δ*galU* cultures. This lysis could be due to the altered lipid A component in the Δ*waa* mutants as described above. Lipid A attaches LPS to the bacterial outer membrane; and therefore, contributes to outer membrane integrity. Lipid A has been found to reduce outer membrane permeability as an improved defense mechanism against the innate immune system in *P. aeruginosa* [43]. Thus, the altered lipid A in the Δ*waa* mutants could have resulted in increased membrane permeability resulting in cell death in the presence of bile salts.

Key differences between Δ*waaG* and Δ*waaJ* include the bacteriostatic response of Δ*waaG* in TSB + 0.4% bile salts; and thus an insufficient bacterial pellet for LPS purification. Because Δ*waaJ* was able to yield LPS purified in TSB + bile salts and also have increased growth in TSB + bile salts compared to Δ*waaG,* the outer core length likely impacts bile salts resistance in the presence of glucose. The bacteriostatic effect was not seen in LB + bile salts for

Δ*waaG*, suggesting the increased glucose levels present in TSB could lead to reduced growth kinetics in bile salts. The mutant could potentially try to repair the LPS structure in the combined presence of glucose and bile salts; and thus, not properly utilize glucose for growth. Furthermore, it has been found that a Δ*waaG* mutant in *E.coli* has significantly increased hydrophobicity, suggesting that LPS lacking a significant portion of the outer core can increase the membrane permeability of bacterial cells [71]. With a smaller outer core in Δ*waaG* compared to Δ*waaJ,* a more permeable membrane and higher susceptibility to bile salts could result. Neither Δ*waa* mutant reached WT levels of growth in bile salts media, indicating that the mutants cannot fully compensate for the growth defects. The data indicate that LPS with a more complete outer core, if present, is able to better resist bile salts exposure and/or utilize glucose during stressful growth [18 23 24 46 64 71].

Biofilm Solid-Phase Adherence Assays

For *Shigella,* both glucose and bile salts exposure are required for the formation of a biofilm. Glucose provides the necessary energy and materials for production of the extracellular polymeric substance (EPS) matrix, a vital component to biofilms [19 54 55]. *Shigella* releases this EPS matrix in response to bile salts as a form of protection during intestinal transit. Among the mutants, Δ*galU* had the most biofilm formation (**Figure 12**). Future analyses are needed to determine if the biofilm biomass is due to the adherence of the bacteria and/or production of the EPS matrix [54 55]. The *galU* gene is responsible for the synthesis of uridine diphosphoglucose, a glucose molecule in glycosidic linkage with uridine diphosphate involved in LPS biosynthesis (Uniprot [68]). Furthermore, *galU* has been found to be important in the catabolism of exogenous

galactose [53]. Therefore, EPS matrix production in this mutant could be impaired as a result, which has been observed in *V. cholerae* [53]. If some matrix is produced, it is possible that the composition is different relative to WT bacteria. Polysaccharides are the predominant components of the EPS matrix [19]; and therefore, other sugars could potentially compensate for the matrix production. Nevertheless, the mutant still had a significant reduction relative to WT bacteria; and thus, the Δ*galU* deletion also affected biofilm formation. This reduction in biofilm production is despite the eventual recovery in growth of the mutant in bile salts and the alterations to the LPS structure in TSB + bile salts as discussed above.

Interestingly, the Δ*galU* mutant had increased biofilm formation compared to both Δ*waa* mutants. The growth defects of both Δ*waa* mutants certainly impacted biofilm production and is the likely reason why no biofilms were even detected. Additionally, the mutants likely cannot produce the matrix. Literature suggests that UDP-galactose synthesis via UDP-glucose is a necessary step in EPS matrix biosynthesis in *V. cholerae* [53]. The *waaJ* gene encodes UDP-glucose:(galactosyl) LPS alpha1,2-glucosyltransferase that adds glucosyl residues to the LPS core backbone (Kegg [29]); and therefore, the Δ*waaJ* mutant may be unable to adequately produce the EPS matrix. The *waaG* gene encodes LPS alpha1,3-glucosyltransferase, which aids in the addition of the first glucose residue to the LPS core (NCBI Reference Sequence [52]). Because glucose is a necessary component of biofilm formation, it is possible that Δ*waaG* is unable to utilize glucose in EPS biosynthesis as well. Furthermore, with the mutant growth defects in bile salts media, it is possible that the glucose in the media was used for growth and no additional resources were available for biofilm formation.

In order to test whether glucose utilization for growth or LPS truncations has a greater role in biofilm formation, mutants with an intact LPS but inability to utilize glucose can be constructed and analyzed. Additionally, rough LPS mutants (lacking only the Oag) without glucose deficiencies can be analyzed in order to compare EPS matrix production. It is likely that the bacteria utilize both LPS genes and glucose metabolism in order to form a biofilm. The LPS inner core composition plays a role in biofilm formation in *E. coli* [51] in that the sugar composition impacts the ability of the strain to form a biofilm. In *V. cholera*, strains deficient in both inner and outer core structures were found to have heightened sensitivity to bile and other hydrophobic agents, as measured by minimum inhibitory concentration testing [53]. Furthermore, the *galU* mutant in *Vibrio cholera* was unable to form a biofilm, suggesting that UDP-glucose or UDP-galactose is necessary for biosynthesis of the EPS [53]. Thus, future analyses investigating the sugar composition of the LPS inner core would provide more mechanistic insight into the links between LPS and biofilm formation in *S. flexneri.* Finally, the biofilm assays can be modified in the future to further evaluate the LPS mutants. Like the LPS purification and growth analyses, a 1:1 dilution of bacteria can be used in the biofilm assay. Preliminary analysis revealed that this dilution had no effect on the ability of the mutants to form a biofilm. Furthermore, the biofilm analyses could be extended to a 48 hour incubation, instead of 24 hours, to determine if the mutants can compensate over a longer time frame to form a biofilm.

Conclusion

This work reveals the importance of *S. flexneri* LPS in resisting the bactericidal effects of long-term bile salts exposure during small intestinal transit. The results contribute to our understanding of bile salt resistance mechanisms in *S. flexneri* as well as to the literature investigating a broad *Shigella* vaccine. Current vaccine candidates do not consider the effects of bile salts exposure on LPS alterations or the ability of antibodies to recognize such alterations. For a broad *Shigella* vaccine to be successful, it would need to provide coverage against multiple serotypes and consider LPS alterations that occur during host transit. In order to investigate the effects of specific LPS biosynthesis genes on the ability of *Shigella* to resist bile salts, three mutants with truncations in the LPS were evaluated: Δ*galU,* Δ*waaG,* and Δ*waaJ*. LPS visualization analyses showed that bile salts exposure results in modified Oag, lipid A, inner and outer core residues for WT as well as the three mutants. While all three mutants had delayed growth in bile salts media compared to WT, each mutant was able to alter the LPS structure, compensate, and ultimately grow in bile salts. This work suggests that the modifications of individual LPS components and expression of LPS biosynthesis genes are important for small intestinal survival. Future analyses will expand our understanding of the LPS structure in bile salt resistance; and importantly, may help to achieve a successful vaccine that can finally prevent the devastating infection rates of *Shigella*.

Works Cited

1. Ahmed, S., Mohammod, F., Fahmida Dil, J. Das, Ferdous, F., & Jonathan R, J. C. (2015). Shigellosis among Breastfed Children: A Facility Based Observational Study in Rural Bangladesh. Journal of Gastrointestinal & Digestive System, 05(05). https://doi.org/10.4172/2161-069x.1000327

2. Anderson, M. C., Vonaesch, P., Saffarian, A., Marteyn, B. S., & Sansonetti, P. J. (2017). Shigella sonnei Encodes a Functional T6SS Used for Interbacterial Competition and Niche Occupancy. Cell Host and Microbe, 21(6), 769-776.e3. https://doi.org/10.1016/j.chom.2017.05.004

3. Ashida, H., Mimuro, H., & Sasakawa, C. (2015). Shigella manipulates host immune responses by delivering effector proteins with specific roles. Frontiers in Immunology. https://doi.org/10.3389/fimmu.2015.00219

4. Barry, E. M., Pasetti, M. F., Sztein, M. B., Fasano, A., Kotloff, K. L., & Levine, M. M. (2013). Progress and pitfalls in Shigella vaccine research. Nature Reviews Gastroenterology and Hepatology. https://doi.org/10.1038/nrgastro.2013.12

5. Bergsbaken, T., Fink, S. L., & Cookson, B. T. (2009). Pyroptosis: Host cell death and inflammation. Nature Reviews Microbiology. https://doi.org/10.1038/nrmicro2070

6. Bonnet, M., & Tran Van Nhieu, G. (2016). How Shigella Utilizes Ca2+ Jagged Edge Signals during Invasion of Epithelial Cells. Frontiers in Cellular and Infection Microbiology, 6, 16. https://doi.org/10.3389/fcimb.2016.00016

7. Borczuk, A. C., And, †, & Goldberg, M. B. (1999). Thymic Independence of Adaptive Immunity to the Intracellular Pathogen Shigella flexneri Serotype 2a. INFECTION AND IMMUNITY (Vol. 67). Retrieved from http://iai.asm.org/

8. Borczuk, A. C., & Goldberg, M. B. (1999). Adaptive Immune Response to Shigella flexneri 2a cydC in Immunocompetent Mice and Mice Lacking Immunoglobulin A. INFECTION AND IMMUNITY (Vol. 67). Retrieved from https://www.ncbi.nlm.nih.gov/pmc/articles/PMC96558/pdf/ii002001.pdf

9. Casabuono, A. C., Van Der Ploeg, C. A., Rogé, A. D., Bruno, S. B., & Couto, A. S. (2012). Characterization of lipid A profiles from Shigella flexneri variant X lipopolysaccharide. Rapid Communications in Mass Spectrometry, 26(17), 2011–2020. https://doi.org/10.1002/rcm.6306

10. Centers for Disease Control and Prevention. (n.d.). Shigella – Shigellosis. Retrieved March 22, 2019, from https://www.cdc.gov/shigella/index.html

11. Daniels, C., & Adelaide, B. S. (1999). Characterisation of proteins involved in Shigella flexneri O-antigen biosynthesis By.

12. Davis, Jr., M. R., & Goldberg, J. B. (2012). Purification and Visualization of Lipopolysaccharide from Gram-negative Bacteria by Hot Aqueous-phenol Extraction. Journal of Visualized Experiments, (63). https://doi.org/10.3791/3916

13. Faherty, C. S., & Maurelli, A. T. (2009). Spa15 of Shigella flexneri is secreted through the type III secretion system and prevents staurosporine-induced apoptosis. Infection and Immunity, 77(12), 5281–5290. https://doi.org/10.1128/IAI.00800-09

14. Faherty, C. S., Redman, J. C., Rasko, D. A., Barry, E. M., & Nataro, J. P. (2012). Shigella flexneri effectors OspE1 and OspE2 mediate induced adherence to the colonic epithelium following bile salts exposure. Molecular Microbiology, 85(1), 107–121. https://doi.org/10.1111/j.1365-2958.2012.08092.x

15. FORMAL, S. B., DAMMIN, G. J., LABREC, E. H., & SCHNEIDER, H. (1958). Experimental Shigella infections: characteristics of a fatal infection produced in guinea pigs. Journal of Bacteriology, 75(5), 604–610. Retrieved from https://www.ncbi.nlm.nih.gov/pmc/articles/PMC290116/pdf/jbacter00512-0129.pdf

16. Gemski, P., Sheahan, D. G., Washington, 0, & Formal, S. B. (1972). Virulence of Shigella flexneri Hybrids Expressing Escherichia coli Somatic Antigens. INFECTION AND IMMUNITY. Retrieved from https://www.ncbi.nlm.nih.gov/pmc/articles/PMC422501/pdf/iai00272-0004.pdf

17. Goldberg, Marcia B., M. (2013). Shigella infection: Epidemiology, microbiology, and pathogenesis, 14–15. Retrieved from http://www.siccordoba.com/cursotrienal/admin/archivos/Shigella infection.pdf

18. Guan, S., Bastint, D. A., & Verma, N. K. (1999). Functional analysis of the 0 antigen glucosylation gene cluster of Shigella flexneri bacteriophage SfX (Vol. 145). Retrieved from www.microbiologyresearch.org

19. Gupta, P., Sarkar, S., Das, B., Bhattacharjee, S., & Tribedi, P. (2016, January 16). Biofilm, pathogenesis and prevention—a journey to break the wall: a review. Archives of Microbiology. Springer Berlin Heidelberg. https://doi.org/10.1007/s00203-015-1148-6

20. Gwen E. Allison, & Naresh K. Verma. (2000). Serotype-converting bacteriophages and O-antigen modification in Shigella flexneri. Trends in Microbiology, 8(1), 17–22. Retrieved from https://pdf.sciencedirectassets.com/271202/1-s2.0-S0966842X00X00479/1-s2.0-S0966842X99016467/main.pdf?x-amz-security-token=FQoGZXIvYXdzEPn%2F%2F%2F%2F%2F%2F%2F%2F%2F%2FwEaDEKQAv5N7XA5zN7A1CK3A6lGThkxdKUDQZxr3zHkqpUOIS3Lku0%2FAU3F0AuNCAyNw8f6Tj2e6goOGbcM5a

21. Hadjifrangiskou, M., Gu, A. P., Pinkner, J. S., Kostakioti, M., Zhang, E. W., Greene, S. E., … Warren, G. (2012). Transposon Mutagenesis Identifies Uropathogenic Escherichia coli Biofilm Factors. https://doi.org/10.1128/JB.01012-12

22. Hoa Tran, E. N., Doyle, M. T., & Morona, R. (2013). LPS Unmasking of Shigella flexneri Reveals Preferential Localisation of Tagged Outer Membrane Protease IcsP to Septa and New Poles. PLoS ONE, 8(7), e70508. https://doi.org/10.1371/journal.pone.0070508

23. Hoa Tran, E. N., Papadopoulos, M., & Morona, R. (2014). Relationship between O-antigen chain length and resistance to colicin E2 in Shigella flexneri. Microbiology (United Kingdom), 160(PART 3), 589–601. https://doi.org/10.1099/mic.0.074955-0

24. Hong, M., & Payne, S. M. (1997). Effect of mutations in Shigella flexneri chromosomal and plasmid-encoded lipopolysaccharide genes on invasion and serum resistance. Molecular Microbiology, 24(4), 779–791. https://doi.org/10.1046/j.1365-2958.1997.3731744.x

25. Humann, J., & Lenz, L. L. (2009). Bacterial peptidoglycan-degrading enzymes and their impact on host muropeptide detection. Journal of Innate Immunity. https://doi.org/10.1159/000181181

26. Jennison, A. V, & Verma, N. K. (2004). Shigella flexneri infection: Pathogenesis and vaccine development. FEMS Microbiology Reviews. https://doi.org/10.1016/j.femsre.2003.07.002

27. Justiz Vaillant, A. A., & Jan, A. (2019). Physiology, Immune Response. StatPearls. StatPearls Publishing. Retrieved from http://www.ncbi.nlm.nih.gov/pubmed/30969623

28. Kamada, N., Chen, G. Y., Inohara, N., & Núñez, G. (2013). Control of pathogens and pathobionts by the gut microbiota. Nature Immunology. https://doi.org/10.1038/ni.2608

29. KEGG PATHWAY Database. (n.d.). Retrieved May 1, 2019, from https://www.genome.jp/kegg/pathway.html

30. Köhler, H., Rodrigues, S. P., & McCormick, B. A. (2002). Shigella flexneri interactions with the basolateral membrane domain of polarized model intestinal epithelium: Role of lipopolysaccharide in cell invasion and in activation of the mitogen-activated protein kinase ERK. Infection and Immunity, 70(3), 1150–1158. https://doi.org/10.1128/IAI.70.3.1150-1158.2002

31. Kong, Q., Yang, J., Liu, Q., Alamuri, P., Roland, K. L., & Curtiss, R. (2011). Effect of Deletion of Genes Involved in Lipopolysaccharide Core and O-Antigen Synthesis on Virulence and Immunogenicity of Salmonella enterica Serovar Typhimurium. Infection and Immunity, 79(10), 4227–4239. https://doi.org/10.1128/iai.05398-11

32. Kotloff, K. L. Shigella infection in children and adults: a formidable foe, 5 The Lancet Global Health § (2017). https://doi.org/10.1016/S2214-109X(17)30431-X

33. Kotloff, K. L., Nataro, J. P., Blackwelder, W. C., Nasrin, D., Farag, T. H., Panchalingam, S., … Levine, M. M. (2013). Burden and aetiology of diarrhoeal disease in infants and young children in developing countries (the Global Enteric Multicenter Study, GEMS): A prospective, case-control study. The Lancet, 382(9888), 209–222. https://doi.org/10.1016/S0140-6736(13)60844-2

34. Kotloff, K. L., Riddle, M. S., Platts-Mills, J. A., Pavlinac, P., & Zaidi, A. K. M. (2018). Shigellosis. The Lancet, 391(10122), 801–812. https://doi.org/10.1016/S0140-6736(17)33296-8

35. Kubatzky, K. F., Agaisse, H., Picking, W., Ashida, H., Mimuro, H., & Sasakawa, C. (2015). Shigella manipulates host immune responses by delivering effector proteins with specific roles. https://doi.org/10.3389/fimmu.2015.00219

36. Le-Barillec, K., Magalhaes, J. G., Corcuff, E., Thuizat, A., Sansonetti, P. J., Phalipon, A., & Di Santo, J. P. (2014). Roles for T and NK Cells in the Innate Immune Response to Shigella flexneri. The Journal of Immunology, 175(3), 1735–1740. https://doi.org/10.4049/jimmunol.175.3.1735

37. Leo, J. C., Grin, I., & Linke, D. (2012). Type V secretion: Mechanism(S) of autotransport through the bacterial outer membrane. Philosophical Transactions of the Royal Society B: Biological Sciences. https://doi.org/10.1098/rstb.2011.0208

38. Lichtman, A. Pillai, S. Abbas, A. (2008). Cellular and Molecular Immunology. Postgraduate Medical Journal, 68(798), 305–305. https://doi.org/10.1136/pgmj.68.798.305

39. Lin, J., Smith, M. A., Benjamin, W. H., Kaminski, R. W., Wenzel, H., & Nahma, M. H. (2016). Monoclonal antibodies to Shigella lipopolysaccharide are useful for vaccine production. Clinical and Vaccine Immunology, 23(8), 681–688. https://doi.org/10.1128/CVI.00148-16

40. Liszewski, M.K, & Atkinson, J. P. (2015). Complement regulators in human disease: Lessons from modern genetics. Journal of Internal Medicine, 277(3), 294–305. https://doi.org/10.1111/joim.12338

41. Livio, S., Strockbine, N. A., Panchalingam, S., Tennant, S. M., Barry, E. M., Marohn, M. E., … Levine, M. M. (2014). Shigella Isolates From the Global Enteric Multicenter Study Inform Vaccine Development. https://doi.org/10.1093/cid/ciu468

42. Macpherson, D. F., Cheah, K.-C., Morona, R., Manning, P. A., & Beger, D. W. (2006). Genetic analysis of the rfb region of Shigella flexneri encoding the Y serotype O-antigen specificity. Molecular Microbiology, 5(6), 1491–1499. https://doi.org/10.1111/j.1365-2958.1991.tb00795.x

43. Maldonado, R. F., Sá-Correia, I., & Valvano, M. A. (2016, July 1). Lipopolysaccharide modification in gram-negative bacteria during chronic infection. (C. Whitfield, Ed.), FEMS Microbiology Reviews. Narnia. https://doi.org/10.1093/femsre/fuw007

44. Mann, M., Olsen, J. V, Tomas, H., Havli\[sbreve], J., & Shevchenko, A. (2007). In-gel digestion for mass spectrometric characterization of proteins and proteomes. Nature Protocols, 1(6), 2856–2860. https://doi.org/10.1038/nprot.2006.468

45. Marteyn, B. S., Gazi, A. D., & Sansonetti, P. J. (2012). Shigella: A model of virulence regulation in vivo. Gut Microbes, 3(2), 104–120. https://doi.org/10.4161/gmic.19325

46. Martinić, M., Hoare, A., Contreras, I., & Álvarez, S. A. (2011). Contribution of the lipopolysaccharide to resistance of Shigella flexneri 2a to extreme acidity. PLoS ONE, 6(10). https://doi.org/10.1371/journal.pone.0025557

47. Mattock, E., & Blocker, A. J. (2017). How Do the Virulence Factors of Shigella Work Together to Cause Disease? Frontiers in Cellular and Infection Microbiology, 7. https://doi.org/10.3389/fcimb.2017.00064

48. Maurelli, A. T., Blackmon, B., & Curtiss, R. (1984). Loss of pigmentation in Shigella flexneri 2a is correlated with loss of virulence and virulence-associated plasmid. Infection and Immunity, 43(1), 397–401. Retrieved from http://www.ncbi.nlm.nih.gov/pubmed/6360906

49. Merritt, M. E., & Donaldson, J. R. (2009). Effect of bile salts on the DNA and membrane integrity of enteric bacteria. Journal of Medical Microbiology. https://doi.org/10.1099/jmm.0.014092-0

50. Müller, E., Hinckley, A., & Rothfield, L. (1972). Studies of phospholipid-requiring bacterial enzymes. 3. Purification and properties of uridine diphosphate glucose:lipopolysaccharide glucosyltransferase I. The Journal of Biological Chemistry, 247(8), 2614–2622. Retrieved from http://www.ncbi.nlm.nih.gov/pubmed/4553445

51. Nakao, R., Ramstedt, M., Wai, S. N., & Uhlin, B. E. (2012). Enhanced Biofilm Formation by Escherichia coli LPS Mutants Defective in Hep Biosynthesis. PLoS ONE, 7(12), 51241. https://doi.org/10.1371/journal.pone.0051241

52. Home - Gene - NCBI. (n.d.). Retrieved May 1, 2019, from https://www.ncbi.nlm.nih.gov/gene

53. Nesper, J., Lauriano, C. M., Klose, K. E., Kapfhammer, D., Kraiß, A., & Reidl, J. (2001). Characterization of Vibrio cholerae O1 El Tor galU and galE mutants: Influence on lipopolysaccharide structure, colonization, and biofilm formation. Infection and Immunity, 69(1), 435–445. https://doi.org/10.1128/IAI.69.1.435-445.2001

54. Nickerson, K. P., Chanin, R. B., Sistrunk, J. R., Rasko, D. A., Fink, P. J., Barry, E. M., … Faherty, C. S. (2017). Analysis of Shigella flexneri Resistance, Biofilm Formation, and Transcriptional Profile in Response to Bile Salts. Infection and Immunity, 85(6), 1–18.

55. Nickerson, K. P., Faherty, C. S. Bile Salt-induced Biofilm Formation in Enteric Pathogens: Techniques for Identification and Quantification. J. Vis. Exp. (135), e57322, doi:10.3791/57322 (2018).

56. Pasqua, M., Grossi, M., Scinicariello, S., Aussel, L., Barras, F., Colonna, B., & Prosseda, G. (2019). The MFS efflux pump EmrKY contributes to the survival of Shigella within macrophages. Scientific Reports, 9(1). https://doi.org/10.1038/s41598-019-39749-3

57. Pastor, Y., Camacho, A. I., Zúñiga-Ripa, A., Merchán, A., Rosas, P., Irache, J. M., & Gamazo, C. (2018). Towards a subunit vaccine from a Shigella flexneri ΔtolR mutant. Vaccine, 36(49), 7509–7519. https://doi.org/10.1016/j.vaccine.2018.10.066

58. Philpott, D. J., Edgeworth, J. D., & Sansonetti, P. J. (2000). The pathogenesis of Shigella flexneri infection: lessons from in vitro and in vivo studies. Retrieved from https://www.ncbi.nlm.nih.gov/pmc/articles/PMC1692768/pdf/10874731.pdf

59. Picking, W. D., Viswanathan, V. K., Mariane, S., Fleiszig, J., Marteyn, B. S., Anderson, M., & Sansonetti, P. J. (2016). Shigella Diversity and Changing Landscape: Insights for the Twenty-First Century. Frontiers in Cellular and Infection Microbiology | Www.Frontiersin.Org, 1, 45. https://doi.org/10.3389/fcimb.2016.00045

60. Rich, R. R., Fleisher, T. A., Sherer, W. T., Schroeder, H. W., Frew, A. J., & Weyand, C. M. (2019). Clinical immunology : principles and practice (5th ed.). Elsevier.

61. Ridlon, J. M., Kang, D.-J., & Hylemon, P. B. (2005). Bile salt biotransformations by human intestinal bacteria. Journal of Lipid Research, 47(2), 241–259. https://doi.org/10.1194/jlr.r500013-jlr200

62. Samandari, T., Kotloff, K. L., Losonsky, G. A., Picking, W. D., Sansonetti, P. J., Levine, M. M., & Sztein, M. B. (2000). Production of IFN- and IL-10 to Shigella Invasins by Mononuclear Cells from Volunteers Orally Inoculated with a Shiga Toxin-Deleted Shigella dysenteriae Type 1 Strain. The Journal of Immunology, 164(4), 2221–2232. https://doi.org/10.4049/jimmunol.164.4.2221

63. Sandlin, R. C., Lampel, K. A., Keasler, S. P., Goldberg, M. B., Stolzer, A. L., & Maurelli, A. T. (1995). Avirulence of rough mutants of Shigella flexneri: Requirement of O antigen for correct unipolar localization of IcsA in the bacterial outer membrane. Infection and Immunity, 63(1), 229–237. Retrieved from http://www.ncbi.nlm.nih.gov/pubmed/7528731

64. Sansonetti, P. J., Arondel, J., Huerre, M., Harada, A., & Matsushima, A. K. (1999). Interleukin-8 Controls Bacterial Transepithelial Translocation at the Cost of Epithelial Destruction in Experimental Shigellosis. INFECTION AND IMMUNITY (Vol. 67). Retrieved from https://www.ncbi.nlm.nih.gov/pmc/articles/PMC96483/pdf/ii001471.pdf

65. Sistrunk, J. R., Nickerson, K. P., Chanin, R. B., Rasko, D. A., & Faherty, C. S. (2016). Survival of the fittest: How bacterial pathogens utilize bile to enhance infection. Clinical Microbiology Reviews, 29(4), 819–836. https://doi.org/10.1128/CMR.00031-16

66. Sperandio, B., Regnault, B., Guo, J., Zhang, Z., Stanley, S. L., Sansonetti, P. J., & Pédron, T. (2008). Virulent Shigella flexneri subverts the host innate immune response through manipulation of antimicrobial peptide gene expression. The Journal of Experimental Medicine, 205(5), 1121–1132. https://doi.org/10.1084/jem.20071698

67. Thanassi, D. G., Cheng, L. W., & Nikaido, H. (1997). Active efflux of bile salts by Escherichia coli. Journal of Bacteriology, 179(8), 2512–2518. https://doi.org/10.1128/jb.179.8.2512-2518.1997

68. UniProt. (n.d.). Retrieved May 1, 2019, from https://www.uniprot.org/

69. University, C. S. (2012). Secretion of Bile and the Role of Bile Acids In Digestion Secretion of Bile and the Role of Bile Acids In Digestion. Vivo Pathophysiology, 2–4. Retrieved from http://www.vivo.colostate.edu/hbooks/pathphys/digestion/liver/bile.html

70. Venkatesan, M. M., Goldberg, M. B., Rose, D. J., Grotbeck, E. J., Burland, V., & Blattner, F. R. (2001). Complete DNA sequence and analysis of the large virulence plasmid of Shigella flexneri. Infection and Immunity, 69(5), 3271–3285. https://doi.org/10.1128/IAI.69.5.3271-3285.2001

71. Wang, Z., Wang, J., Ren, G., Li, Y., & Wang, X. (2015). Influence of core oligosaccharide of lipopolysaccharide to outer membrane behavior of Escherichia coli. Marine Drugs, 13(6), 3325–3339. https://doi.org/10.3390/md13063325

72. Wanner, K. A. D. and B. L. (2000). Escherichia One-step inactivation of chromosomal genes in, xx(xx), 1–7. https://doi.org/10.1016/j.jbiosc.2015.08.006

73. Way, S. S., Borczuk, A. C., & Goldberg, M. B. (1999). Thymic independence of adaptive immunity to the intracellular pathogen Shigella flexneri serotype 2a. Infection and Immunity, 67(8), 3970–3979. Retrieved from http://iai.asm.org/

74. Wei, J., Goldberg, M. B., Burland, V., Venkatesan, M. M., Deng, W., Fournier, G., … Blattner, F. R. (2003). Complete genome sequence and comparative genomics of Shigella flexneri serotype 2a strain 2457T. Infection and Immunity, 71(5), 2775–2786. https://doi.org/10.1128/IAI.71.5.2775-2786.2003